

STLCCP: An Efficient Convex Optimization-based Framework for Signal Temporal Logic Specifications

Yoshinari Takayama, Kazumune Hashimoto, Toshiyuki Ohtsuka

Abstract—Signal Temporal Logic (STL) is capable of expressing a broad range of temporal properties that controlled dynamical systems must satisfy. In the literature, both mixed-integer programming (MIP) and nonlinear programming (NLP) methods have been applied to solve optimal control problems with STL specifications. However, neither approach has succeeded in solving problems with complex long-horizon STL specifications within a realistic timeframe. This study proposes a new optimization framework, called *STLCCP*, which explicitly incorporates several structures of STL to mitigate this issue. The core of our framework is a structure-aware decomposition of STL formulas, which converts the original program into a difference of convex (DC) programs. This program is then solved as a convex quadratic program sequentially, based on the convex-concave procedure (CCP). Our numerical experiments on several commonly used benchmarks demonstrate that this framework can effectively handle complex scenarios over long horizons, which have been challenging to address even using state-of-the-art optimization methods.

Index Terms—Convex optimization, optimal control, formal methods, signal temporal logic

I. INTRODUCTION

Autonomous robotic systems, such as self-driving cars, drones, and cyber-physical systems, are expected to have extensive real-world applications in transportation, delivery, and industrial automation in the near future. These systems must perform complex control tasks while ensuring safety, ideally with formal guarantees. In response to this need, researchers have developed formal specification languages that offer a unified and rigorous approach to expressing complex requirements for safe and reliable autonomous systems. One such language is signal temporal logic (STL) [1], which is well-suited for continuous real-valued signals. It offers a useful quantitative semantics called *robustness* [2], which quantifies how robustly a formula is satisfied. By maximizing this score, control input sequences can be synthesized robustly, and the resulting trajectories can formally satisfy the specification. However, precisely formulating this optimization problem as a mixed-integer program (MIP) is known to be problematic in terms of scalability with respect to the length of the horizon.

To avoid this issue, recent work has focused on formulating the problem as nonlinear programs (NLP) by smooth approximations of the max and min operators in the robustness

function [3, 4, 5]. These NLP are then solved *naively* through a sequential quadratic programming (SQP) method (or other gradient-based methods). While these SQP-based methods are generally faster and more scalable than MIP-based methods, their major drawback is that they can easily become infeasible and may not find the global optima due to the iterative approximations. For instance, the traditional SQP method approximates the original problem to a quadratic program, which retains only up to the second derivative information of the original problem. This drawback can become even more pronounced when problem structures are not exploited. Specifically, in control problems with STL specifications, the non-convex robustness function in the cost function is frequently coarsely approximated by the traditional SQP method.

This study aims to tackle these issues by explicitly incorporating several *structures of STL*. To accomplish this, we introduce a novel optimization framework, called *STLCCP*, which uses the convex-concave procedure (CCP) [6, 7] for iterative optimization. The *STLCCP* framework can handle *any* STL specifications and consists of three steps: the preparation step, the reformulation step, and the solving step (refer to Algorithm 3). In contrast to the conventional SQP method, the proposed framework retains complete information of convex parts at each iteration, resulting in fewer approximations. Furthermore, it is designed to be computationally efficient: when the system satisfies the linearity assumption, it solves quadratic programs sequentially, with only disjunctive parts of the specification being linearized at each iteration. Although we mainly focus on the linear case to demonstrate the theoretical validity of our approach, our framework can handle the general nonlinear case where it becomes a method that solves non-quadratic convex programs sequentially. Open-source code is available at <https://github.com/yotakayama/STLCCP>.

A. Contributions

The contributions of this paper are multi-fold as follows.

- i) To introduce the idea of the CCP for control problems with STL specifications, we propose a new *robustness decomposition* framework, which converts the robustness function into a set of constraints systematically. By considering the structures of STL, this decomposition reduces the non-convex parts of the program and makes the convex parts quadratic (or linear). As a result, *STLCCP* becomes an efficient SQP (CCP-based SQP) method.
- ii) To guide the optimization steps not to neglect the *important* constraints, we improve the CCP-based algorithm further by prioritizing those constraints. This method, termed *tree-weighted penalty CCP (TWP-CCP)*, leverages the hierarchical nature of STL by exploiting the structure of the reformulated program.

Y. Takayama is with University Paris-Saclay, CNRS, CentraleSupélec, Laboratory of Signals and Systems (L2S), Gif-sur-Yvette, France. K. Hashimoto is with the Graduate School of Engineering, Osaka University, Osaka, Japan. T. Ohtsuka is with the Graduate School of Informatics, Kyoto University, Kyoto, Japan. Corresponding author: Yoshinari Takayama. This work was completed when the first author was at Kyoto University. This work was partially supported by JSPS KAKENHI under Grant JP22H01510 and 21K14184, by JST CREST under Grant JPMJCR201, and by Watanabe Foundation. Email: (yoshinari.takayama@l2s.centralesupelec.fr, hashimoto@eei.eng.osaka-u.ac.jp, ohtsuka@i.kyoto-u.ac.jp)

- iii) We propose a new smooth robustness measure that is suitable for our framework using a novel smoothing function, which we call a *mellowmin* function. This robustness has not only soundness and asymptotic completeness properties, but also the tradeoff between the roughness of the majorization and the completeness of the smooth approximation. Additionally, we propose a warm start approach for the efficient utilization of this measure in practice.
- iv) The results of our numerical experiments on several benchmarks indicate that our proposed method outperforms state-of-the-art methods in terms of both robustness score and computational time.

B. Key feature of our framework

One of the key features of our framework is its ability to exploit the structures of STL specifications. These structures can be divided into three categories: first, all the logical operators in STL specifications, including temporal operators, can be integrally explained using the terms *conjunctive* or *disjunctive*, corresponding to the max or min functions of robustness function, second, the robustness function has a *monotonicity property*, and third, the logical operators in an STL specification have a *hierarchical tree structure*. In the following, we elaborate on how our framework exploits these three properties:

Conjunctive-disjunctive to convex-concave: We formally establish a *correspondence* between conjunctive and disjunctive operators and the convexity or concavity of the optimization program. This allows us to reformulate the problem into a DC program by mapping conjunctive operators to convex parts of the program and disjunctive operators to concave parts (see Section II).

Monotonicity property: We utilize the monotonicity property to make the reformulation more rigorous and precise. This precise reformulation of the original problem into a DC program minimizes information loss due to approximations (see Section IV).

Hierarchical structure: We exploit the information of *priority ranking* among the constraints to avoid significant violations of important constraints in a hierarchical manner (see Section VI). The literature has not utilized this priority ranking among the nodes although some papers also viewed STL as a tree. This is because the naive formulation makes it difficult to differentiate the importance of each node. However, we overcome this challenge through the reformulation.

In addition to the hierarchical priority structure, the perspective of viewing the robustness function as a tree is important throughout this paper and is utilized in many ways. For instance, we apply the formula simplification technique in [8] to reduce the part that we approximate at each step.

C. Related works

Control under temporal logic specifications: Traditionally, approaches based on the abstraction of models have been effective in solving the trajectory synthesis problem under temporal logic specifications. However, they require a

significant amount of domain expertise that is difficult to be automated. Another class of trajectory synthesis algorithms for this problem is the optimization-based approach. While the early papers [9, 10] consider linear temporal logic (LTL) and metric temporal logic (MTL), recent work considers STL specifications [11, 12] as it is more suited to robotic systems with continuous states. Most of these studies have focused on either developing a new metric of robustness [13, 14] or proposing an efficient technique for a specific class of temporal logic specifications [12]. However, these works did not leverage the structure of STL for optimization algorithms. Although there has been recent research that attempts to exploit the tree structure of STL to enhance MIP-based optimization algorithms, such as [8] which reduces the number of integer variables or [15] which proposes a new encoding method for multi-agent problems, these methods do not aim to improve NLP-based algorithms and do not comprehensively use the structures of STL as in this study.

Control using convex optimizations: Convex optimization-based frameworks, such as CCP, have been applied in the field of optimal control in some papers, such as [16, 17]. Recently, these frameworks have also been applied in interdisciplinary research between formal methods and control theory. For example, [18] considered parameter synthesis problems in MDPs, and [19] derived the invariant barrier certificate condition for unbounded time safety. Despite the recent popularity of convex optimization, its application to STL specifications has not yet been explored extensively, although several convex optimization-based frameworks for STL specifications are available, such as [20, 21]. While [20] focuses on the decomposition of global STL specifications assigned to multi-agent systems into local STL tasks, our framework addresses the trajectory synthesis problem for a single system. Additionally, [21] applied a convex optimization-based approach for STL specifications, but their solver had to constrain the updates within a trust region, unlike CCP-based approaches, and their approximated parts are completely different from ours.

Furthermore, there has been no previous work that applies the CCP to control problems with STL specifications, except for the conference version of this paper [22], which essentially corresponds to the contribution presented in Subsection I-A (i). However, the robustness decomposition approach presented in this paper is applicable to a wider range of STL specifications than the simple specification considered in [22]. Furthermore, all contributions listed in Subsection I-A (ii) and (iii) are not covered in the conference paper.

D. Organization of this paper

Section II first introduces the preliminaries and the problem statement. Section III presents two concepts that help us establish a clear connection between convex optimization and formal specifications: a reversed version of the robustness function and its tree structure. Section IV presents our robustness decomposition method that transforms the optimization problem into a non-smoothed DC form. Section V then introduces a new smooth function that fits our convex optimization framework. Section VI proposes the tree-weight penalty CCP

to solve the reformulated DC program. Section VII provides numerical experiments, and Section VIII concludes our paper.

Notations: \mathbb{R} and \mathbb{Z} are defined as the sets of real and integer numbers, respectively. Given $a, b \in \mathbb{Z}$ with $a < b$, $[a, b]$ denotes a set of integers from a to b . True and false are denoted by \top and \perp , respectively, **while the superscript \top indicates transpose**. I_n denotes the identity matrix of size n . $0_{n \times m}$ denotes the zero matrix of size $n \times m$. **In this paper, a signal, or trajectory, is defined as a finite sequence $\mathbf{x} = x_0 x_1 \cdots x_T$, where $x_t \in \mathbb{R}$, $t \in \mathbb{N}$, and $T \in \mathbb{N}$ is referred to as the trajectory length. Trajectories starting at timestep t , i.e., $x_t x_{t+1} \cdots$, are denoted as (\mathbf{x}, t) .**

II. PRELIMINARIES

A. Signal temporal logic (STL)

STL is a predicate logic used to specify properties of trajectories \mathbf{x} . The syntax of negation-free STL is [25]:

$$\varphi := \mu \mid \vee \varphi \mid \wedge \varphi \mid \square_{[t_1, t_2]} \varphi \mid \diamond_{[t_1, t_2]} \varphi \mid \mathbf{U}_{[t_1, t_2]} \varphi_1 \varphi_2,$$

where $\mu = (g^\mu(x_t) \leq 0)$, $g^\mu : \mathbb{R}^n \rightarrow \mathbb{R}$ is a predicate, and the symbol \mid stands for OR and the definition is recursive. In addition to the standard boolean operators \wedge and \vee , the STL also incorporates temporal operators \square (*always*), \diamond (*eventually*), and \mathbf{U} (*until*). In this paper, \wedge and \square are referred to as conjunctive operators. Similarly, \vee and \diamond are referred to as disjunctive operators. Each temporal operator has associated bounded time interval $[t_1, t_2]$ where $0 \leq t_1 < t_2$ and $t_2 < \infty$. Any STL formula can be brought into negation normal form (NNF), where the negations are solely present in front of the predicates [23, 24]. This paper deliberately omits negations from the STL syntax for the later explanation. For simplicity, we refer to this negation-free STL as STL.

The concept of *robustness* is a significant semantics defined for STL formulas, which is a real-valued function that characterizes how well a trajectory satisfies an STL formula. The original robustness of an STL formula φ with respect to a trajectory \mathbf{x} and a time t can be obtained recursively by the quantitative semantics [2]:

$$\begin{aligned} \rho_{\text{orig}}^\mu((\mathbf{x}, t)) &= -g^\mu(x_t) \\ \rho_{\text{orig}}^{\varphi_1 \wedge \varphi_2}((\mathbf{x}, t)) &= \min(\rho_{\text{orig}}^{\varphi_1}((\mathbf{x}, t)), \rho_{\text{orig}}^{\varphi_2}((\mathbf{x}, t))) \\ \rho_{\text{orig}}^{\varphi_1 \vee \varphi_2}((\mathbf{x}, t)) &= \max(\rho_{\text{orig}}^{\varphi_1}((\mathbf{x}, t)), \rho_{\text{orig}}^{\varphi_2}((\mathbf{x}, t))) \\ \rho_{\text{orig}}^{\square_{[t_1, t_2]} \varphi}((\mathbf{x}, t)) &= \min_{t' \in [t+t_1, t+t_2]} (\rho_{\text{orig}}^\varphi((\mathbf{x}, t'))) \\ \rho_{\text{orig}}^{\diamond_{[t_1, t_2]} \varphi}((\mathbf{x}, t)) &= \max_{t' \in [t+t_1, t+t_2]} (\rho_{\text{orig}}^\varphi((\mathbf{x}, t'))) \\ \rho_{\text{orig}}^{\varphi_1 \mathbf{U}_{[t_1, t_2]} \varphi_2}((\mathbf{x}, t)) &= \min_{t' \in [t+t_1, t+t_2]} \left(\max \left(\left[\rho_{\text{orig}}^{\varphi_1}((\mathbf{x}, t')), \right. \right. \right. \\ &\quad \left. \left. \left. \max_{t'' \in [t+t_1, t']} (\rho_{\text{orig}}^{\varphi_2}((\mathbf{x}, t''))) \right] \right) \right) \end{aligned} \quad (1)$$

By maximizing the robustness $\rho_{\text{orig}}^\varphi$ that results from (1), a robust control input sequence can be synthesized. The trajectory length T has to be chosen so that it is longer than the *formula length* of φ , which is the horizon needed to calculate the robustness of a formula (see e.g. [24] for the recursive

calculation of formula lengths). The original robustness is sound in the sense that

$$\rho_{\text{orig}}^\varphi(\mathbf{x}) \geq 0 \implies \mathbf{x} \models \varphi, \quad (2)$$

and also complete in the sense that $\rho_{\text{orig}}^\varphi(\mathbf{x}) < 0 \implies \mathbf{x} \not\models \varphi^1$. Thanks to these properties, the robustness value plays a role as an indicator of how much margin we have until the border between satisfaction and violation.

B. Convex-concave procedure (CCP)

The CCP [7] is a heuristic iterative algorithm to find a local optimum of a class of optimization problems called difference of convex (DC) programs, which is composed of a class of functions called differences of convex (DC) functions:

Definition 1: [6] A function $p : \mathbb{R}^n \rightarrow \mathbb{R}$ is a DC function if there exist convex functions $q, r : \mathbb{R}^n \rightarrow \mathbb{R}$ such that p is expressed as the difference between q and r , i.e., $p(\mathbf{x}) = q(\mathbf{x}) - r(\mathbf{x})$, $\mathbf{x} \in \mathbb{R}^n$.

The broad class of DC functions includes all C^2 functions.

Definition 2: [6] Programs are DC programs if written as:

$$\text{minimize } p_0(\mathbf{z}) \quad (3a)$$

$$\text{subject to } p_i(\mathbf{z}) \leq 0, \quad i \in \{1, \dots, m\}, \quad (3b)$$

where $\mathbf{z} \in \mathbb{R}^h$ is the vector of h optimization variables and $p_i = q_i - r_i : \mathbb{R}^h \rightarrow \mathbb{R}$, $i \in \{0, \dots, m\}$ are DC functions.

The class of DC programs is broad; the almost only condition imposed on the program is merely to know whether each function is convex or concave. Thus, once they are known, a wide range of nonconvex programs become DC programs.

Remark 1: DC problems also includes equality constraints

$$q_i(\mathbf{z}) = r_i(\mathbf{z}), \quad (4)$$

where q_i and r_i are convex. These equality constraints are expressed as the pair of inequality constraints $q_i(\mathbf{z}) - r_i(\mathbf{z}) \leq 0$ and $r_i(\mathbf{z}) - q_i(\mathbf{z}) \leq 0$.

The CCP involves two steps: a majorization step, where concave terms are replaced with a convex upper bound, and a minimization step, where the resulting convex problem is solved. In this study, we adopt the simplest form of majorization, which is linearization at the current point at each iteration. Specifically, the CCP linearizes all non-affine concave functions $-r_i(\mathbf{x})$ in (3):

- i) function $r_0(\mathbf{z})$ in the cost (3a);
- ii) functions $r_i(\mathbf{z})$ in inequality constraints (3b);
- iii) functions $q_i(\mathbf{z})$ and $r_i(\mathbf{z})$ in equality constraints (4),

Remark 2: It is worth noting that both non-affine convex functions $q_i(\mathbf{z})$ and $r_i(\mathbf{z})$ in equality constraints (4) have to be approximated as in Remark 1. This contrasts with the handling of inequality constraints and suggests avoiding equality constraints in CCP whenever possible.

The CCP possesses nice properties, such as (i) all of the iterates are feasible if the starting point is in the feasible set

¹Throughout this paper, we use *soundness* to describe when a robustness value can guarantee the satisfaction of a formula, as in (2). On the other hand, we use *completeness* to describe when a robustness value can also guarantee the violation of a formula.

and (ii) the cost value converges (possibly to negative infinity). See [6, 27] for a proof. Thus, it does not need to restrict the update at each iteration (nor to perform a line search), contrary to the traditional SQP methods that often constrain the update within trust regions. Moreover, CCP often converges within fewer iterations than traditional SQP methods.

C. Problem

We consider nonlinear systems

$$x_{t+1} = f(x_t, u_t), \quad (5)$$

where $f : \mathcal{X} \times \mathcal{U} \rightarrow \mathcal{X}$, $x_t \in \mathcal{X} \subseteq \mathbb{R}^n$ and $u_t \in \mathcal{U} \subseteq \mathbb{R}^m$ are the state and control input at time t . \mathcal{X} and \mathcal{U} are defined by inequalities $h_x(x_t) \leq 0$ and $h_u(u_t) \leq 0$, respectively. Now we formulate the control problem of nonlinear systems (5) with any STL specifications φ in Problem 1, under the following mild assumption.

Assumption 1: The functions f , h_x , and h_u in (5), as well as the functions g^μ for all predicates μ of φ , are DC functions.

Remark 3: In Section I-B, we narrow the class in order to provide useful properties.

Problem 1: Given an initial state x_0 , nonlinear systems (5), and any STL specification φ , find the trajectory \mathbf{x} that satisfies φ (robustly):

$$\min_{\mathbf{x}, \mathbf{u}} -\rho_{\text{orig}}^\varphi(\mathbf{x}) \quad (6a)$$

$$\text{s.t. } x_{t+1} = f(x_t, u_t) \quad (6b)$$

$$x_t \in \mathcal{X}, u_t \in \mathcal{U} \quad (6c)$$

$$\rho_{\text{orig}}^\varphi(\mathbf{x}) \geq 0 \quad (6d)$$

Remark 4: Although we omit quadratic cost terms (such as those in the LQR setting), output equations, and other variables such as disturbances for simplicity, the proposed method can still be applied to such cases if the resulting program is a DC program. Furthermore, it is not necessary to include the robustness function in the cost (6a) for our method. In such cases, the program seeks a satisfactory trajectory without maximizing robustness.

III. USEFUL CONCEPTS FOR OUR PERSPECTIVE

A. Robustness flipping

We first introduce a reversed version of the robustness, denoted ρ_{rev} , which is defined as follows.

Definition 3: (Reversed robustness)

$$\rho_{\text{rev}}^\mu((\mathbf{x}, t)) = g^\mu(x_t) \quad (7a)$$

$$\rho_{\text{rev}}^{\varphi_1 \wedge \varphi_2}((\mathbf{x}, t)) = \max(\rho_{\text{rev}}^{\varphi_1}((\mathbf{x}, t)), \rho_{\text{rev}}^{\varphi_2}((\mathbf{x}, t))) \quad (7b)$$

$$\rho_{\text{rev}}^{\varphi_1 \vee \varphi_2}((\mathbf{x}, t)) = \min(\rho_{\text{rev}}^{\varphi_1}((\mathbf{x}, t)), \rho_{\text{rev}}^{\varphi_2}((\mathbf{x}, t))) \quad (7c)$$

$$\rho_{\text{rev}}^{\square_{[t_1, t_2]} \varphi}((\mathbf{x}, t)) = \max_{t' \in [t+t_1, t+t_2]} (\rho_{\text{rev}}^\varphi((\mathbf{x}, t'))) \quad (7d)$$

$$\rho_{\text{rev}}^{\diamond_{[t_1, t_2]} \varphi}((\mathbf{x}, t)) = \min_{t' \in [t+t_1, t+t_2]} (\rho_{\text{rev}}^\varphi((\mathbf{x}, t'))) \quad (7e)$$

$$\rho_{\text{rev}}^{\varphi_1 \mathbf{U}_{[t_1, t_2]} \varphi_2}((\mathbf{x}, t)) = \max_{t' \in [t+t_1, t+t_2]} \left(\min_{t'' \in [t+t_1, t'']} (\rho_{\text{rev}}^{\varphi_1}((\mathbf{x}, t''))), \min_{t'' \in [t+t_1, t'']} (\rho_{\text{rev}}^{\varphi_2}((\mathbf{x}, t''))) \right) \quad (7f)$$

In the above definition, we reverse the sign of the robustness functions of predicates μ in (7a), and we interchange the max functions and the min functions in (7b)–(7f) from the original robustness ρ_{orig} . The reversed robustness ρ_{rev} satisfies the equation $\rho_{\text{rev}}^\varphi = -\rho_{\text{orig}}^\varphi$. Although this modification may seem redundant as it does not alter the original robustness properties, we introduce it for several reasons. First, it establishes a clear relationship between temporal logic operator types (conjunctive or disjunctive) and optimization constraint curvatures (convex or concave). Table I summarizes this relationship, which will be important throughout the paper. It says that in the reversed version, satisfying conjunctive operators leads to satisfying a convex constraint. As an intuitive example, consider a formula $\varphi = \varphi_1 \wedge \varphi_2$, where φ_1 and φ_2 are linear predicates. When using the reversed robustness $\rho_{\text{rev}}^\varphi$, the constraint is $\max(g^{\varphi_1}, g^{\varphi_2}) \leq 0$. On the other hand, when using the original robustness, it is $-\min(-g^{\varphi_1}, -g^{\varphi_2}) \leq 0$.

TABLE I: Correspondance in the reversed robustness.

node-type	operator	functions	constraints
conjunctive	\wedge, \square	max	convex
disjunctive	\vee, \diamond	min	concave

Secondly, by using this definition, we can avoid maximization formulations, which are not commonly used in the field of convex optimization to avoid confusion. As this paper alternates between the perspectives of temporal logic and convex optimization, this will help the intuitive understanding of the connection. Lastly, employing this reversed definition can simplify the decomposition procedure, which will be discussed in Section 5.

B. Tree structure

Next, we introduce a tree structure for STL formulas, namely a *robustness tree* \mathcal{T}^φ , which is defined for the reversed robustness functions $\rho_{\text{rev}}^\varphi$ constructed from Definition 3. While the authors of [8, 15, 26] also define a tree structure of STL formulas, their motivations differ slightly from ours: [8, 15] focus on MIP-based formulations, while [26] concentrates on back-propagation for learning methods. It is worth noting that our tree structure is defined directly to the reversed robustness function, rather than to the formula.

Definition 4: (Robustness Tree) A robustness tree \mathcal{T}^φ is a tuple $(\mathcal{O}, \mathcal{A}, \mathcal{S})$ corresponding to reversed robustness function $\rho_{\text{rev}}^\varphi$, where

- i) $\mathcal{O} \in \{\max, \min\}$ is the type of the top node of the tree \mathcal{T}^φ , which corresponds to the outermost operator of robustness function $\rho_{\text{rev}}^\varphi$;
- ii) $\mathcal{A} = [\mathcal{T}^{\varphi_1}, \mathcal{T}^{\varphi_2}, \dots, \mathcal{T}^{\varphi_N}]$ is a list of N subtrees (i.e., children) sprouted from the top node, which corresponds to each argument (function) of robustness function $\rho_{\text{rev}}^\varphi$;
- iii) $\mathcal{S} = [t^{\varphi_1}, t^{\varphi_2}, \dots, t^{\varphi_N}]$ is a list of time steps of each subtree. t^{φ_1} and t^{φ_N} correspond to the subscripts of the temporal operator;

Given a robustness function $\rho_{\text{rev}}^\varphi$ (or formula φ itself), the robustness tree \mathcal{T}^φ can be built up recursively. An example of the robustness tree is shown in Fig. 1. As we can see, all the

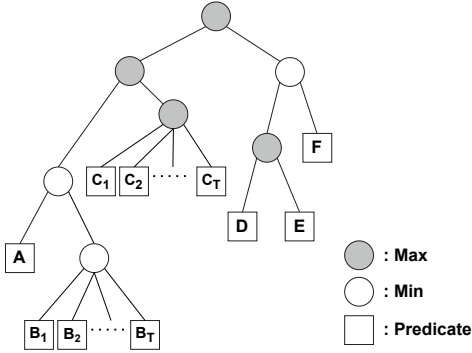


Fig. 1: An example of the robustness tree for formula $\varphi = ((A \vee \diamond_{[1,T]} B) \wedge \square_{[1,T]} C) \wedge ((D \wedge E) \vee F)$, where A, B, C, D, E, F denotes predicates. The grey circles are expressing the max operators, whereas the white circles are expressing the min-type operators. The square boxes are expressing predicates.

bottom nodes of a robustness tree, which we call *leaves*, are predicates. Moreover, all the subtrees in a robustness tree are themselves robustness trees. Thus, every node in a robustness tree is either a max-type node or a min-type node, except for the bottom nodes. As these max-type nodes (resp. the min-type nodes) in the robustness tree correspond to \wedge and \square (resp. \vee and \diamond) from Definition 3, they are sometimes referred as conjunctive nodes (resp. disjunctive nodes). In this sense, \wedge and \square (resp. \vee and \diamond) are treated similarly. On the other hand, the until operator \mathcal{U} does not correspond to a single node as it consists of a conjunction of the max and min functions. It corresponds to a tree whose top node is max-type, whose child nodes are min-type nodes, and whose child nodes are min-type nodes or predicates.

For the later discussion, given a robustness tree of \mathcal{T}^φ , we denote the number of nodes whose operator type is min as N_{\vee}^φ (which correspond to the disjunctive operators in STL formulas) and denote the number of leaves (predicates) as N_p^φ . Also, we denote the number of leaves whose parent node is max type as $N_{p\wedge}^\varphi$, and min type as $N_{p\vee}^\varphi$ where $N_p^\varphi = N_{p\wedge}^\varphi + N_{p\vee}^\varphi$ holds.

Example 1: Consider the formula in Fig.1, i.e., $\varphi = ((A \vee \diamond_{[1,T]} B) \wedge \square_{[1,T]} C) \wedge ((D \wedge E) \vee F)$. There are three max-type trees (associated with robustness trees \mathcal{T}^φ , $\mathcal{T}^{D \vee E}$ and $\mathcal{T}^{(A \vee \diamond_{[1,T]} B) \wedge \square_{[1,T]} C}$), three min-type trees (associated with robustness trees $\mathcal{T}^{A \vee \diamond_{[1,T]} B}$, $\mathcal{T}^{\diamond_{[1,T]} B}$ and $\mathcal{T}^{(D \wedge E) \vee F}$), and $2T + 4$ predicates. Hence, $N_{\vee}^\varphi = 3$, $N_p^\varphi = 2T + 4$. Trees \mathcal{T}^φ , $\mathcal{T}^{A \vee \diamond_{[1,T]} B}$, and $\mathcal{T}^{\diamond_{[1,T]} B}$ has 2, 2, and T subtrees respectively and their lists of time steps are $[0, 0]$, $[0, 0]$, and $[0, 1, \dots, T]$ respectively.

IV. ROBUSTNESS DECOMPOSITION

A. Basic idea of our robustness decomposition

In this section, we present the basic idea of our robustness decomposition. The goal of our decomposition is to turn the problem into a DC program in order to apply a CCP-based algorithm. To this end, we need to know whether each function in the program (6) is convex or concave. In this program (6), the robustness function $\rho_{\text{orig}}^\varphi$ is the only part whose curvature

(convex or concave) cannot be determined. Thus, if the robustness function, which is a composite function consisting of the max and min functions, can be rewritten as a combination of convex and concave functions, the entire program can be reduced to a DC program. The proposed framework achieves this by recursively decomposing the outermost operator of the robustness function using new variables. According to the composition rule in Appendix A, the max and min functions are needed to be decomposed until their arguments become all affine in order to know convex or concave. If the arguments of a function are all predicates, the operator in front of it can be either a max or min function. The recursive decomposition of a nonconvex robustness function into predicates corresponds to a decomposition of the robustness tree from the top to the bottom, in accordance with the tree structure.

The proof of the following theorem shows a naive and elementary procedure for the robustness decomposition, which reformulates Problem 1 into a DC problem.

Theorem 1: The program (6) can be equivalently transformed into a difference of convex (DC) program.

Proof. We constructively prove the statement. As the robustness function is in the cost function, the first procedure is to decompose the function from the cost function into a set of constraints. We describe the procedure for both cases where the outermost operator of the robustness function $\rho_{\text{rev}}^\varphi$ is max and min. If the outermost operator is max, i.e., $\rho_{\text{rev}}^\varphi = \max(\rho_{\text{rev}}^{\varphi_1}, \rho_{\text{rev}}^{\varphi_2}, \dots, \rho_{\text{rev}}^{\varphi_r})$, we replace the cost function with variable s_ξ , and add the constraint

$$\max(\rho_{\text{rev}}^{\varphi_1}, \rho_{\text{rev}}^{\varphi_2}, \dots, \rho_{\text{rev}}^{\varphi_r}) = s_\xi. \quad (8)$$

If the outermost operator is min, i.e., $\rho_{\text{rev}}^\varphi = \min(\rho_{\text{rev}}^{\varphi_1}, \rho_{\text{rev}}^{\varphi_2}, \dots, \rho_{\text{rev}}^{\varphi_r})$, we replace the cost function with variable s_ξ and add the constraint

$$\min(\rho_{\text{rev}}^{\varphi_1}, \rho_{\text{rev}}^{\varphi_2}, \dots, \rho_{\text{rev}}^{\varphi_r}) = s_\xi. \quad (9)$$

After the first decomposition above, the robustness function in the cost is now decomposed into the constraint of the form, either (8) or (9). Note that the arguments of both max and min functions in the constraints are still not necessarily predicates. We continue the same kind of replacement until all the arguments in each function become the predicates: for the constraint of max-form (8), we check whether each argument of the max function is a predicate or not. If all these functions are predicates, we do not have to do any additional steps because function φ is determined to be the concave function from the composition rule in Appendix A. However, if not, we cannot decide whether the term is concave or not. Thus, in this case, we replace each argument that is not a predicate, $\rho_{\text{rev}}^{\varphi_i}$, with a variable s_{new} as $\max(\rho_{\text{rev}}^{\varphi_1}, \dots, s_{\text{new}}, \dots, \rho_{\text{rev}}^{\varphi_r})$. Then we add the equality constraint $\rho_{\text{rev}}^{\varphi_i} = s_{\text{new}}$, which is of the form either (8) or (9). The procedure for the constraint of min-form (9) is the same as the case of (8) above. After applying these replacements for all the non-predicate arguments, all the new constraints are again of the form either (8) or (9). We repeat this procedure until we reach the predicates, the bottom of the STL tree.

When we finish the above recursive manipulations, all the output constraints are of the form either (8) or (9), and the arguments of all max and min functions become affine. Thus, from the composition rule (Appendix A), the curvature (convex or concave) of max and min functions are known. This concludes the proof. \square

B. Fewer non-convex parts via recursive epigraphic reformulations

While the naive decomposition method outlined above is easy to understand, it fails to fully leverage the structure of the problem. Specifically, because all new constraints (8) and (9) take the form of *nonaffine equality*, when they are encoded as two inequality constraints as detailed in Subsection II-B, the number of concave constraints needlessly increases. As each step requires more approximations on those concave terms, this would result in either a large number of iterations or an unsatisfactory local solution. Therefore, it is preferable to reduce the non-convex parts of the program to minimize the iterative approximation by the algorithm. To this end, the rest of the section is devoted to introducing a more elaborated reformulation procedure by using the monotonicity property of STL. After introducing this procedure, we show that this reformulation is *equivalent*². Procedure 1 below uses the idea of the epigraphic reformulation methods, which transform the convex (usually linear) cost function into the corresponding epigraph constraints. However, our approach is different from the normal epigraphic reformulation-based approach in the sense that we deal with *nonconvex* cost functions and we have to apply reformulation *recursively*.

Procedure 1: (Part i. From cost to constraints) To extract the robustness function from the cost function, the initial step involves decomposing the function into a series of constraints. This process varies depending on whether the outermost operator of the robustness function $\rho_{\text{rev}}^{\varphi}$ is a max or min, which is described in **(i. max)** and **(i. min)**, respectively as follows. Note that the max cases are generally simpler than the min cases.

(i. max) We first consider the case when the outermost operator of $\rho_{\text{rev}}^{\varphi}$ is max, i.e., $\rho_{\text{rev}}^{\varphi} = \max(\rho_{\text{rev}}^{\varphi_1}, \rho_{\text{rev}}^{\varphi_2}, \dots, \rho_{\text{rev}}^{\varphi_r})$. In this case, we introduce a new variable s_{ξ} , and reformulate the program as follows:

$$\min_{\mathbf{x}, \mathbf{u}, s_{\xi}} s_{\xi} \quad (10a)$$

$$\text{s.t. (6b), (6c)} \quad (10b)$$

$$s_{\xi} \leq 0 \quad (10c)$$

$$\rho_{\text{rev}}^{\varphi_1}(\mathbf{x}) \leq s_{\xi} \dots \rho_{\text{rev}}^{\varphi_r}(\mathbf{x}) \leq s_{\xi} \quad (10d)$$

(i. min) Next, we consider the case when the outermost operator of $\rho_{\text{rev}}^{\varphi}$ is min, i.e., $\rho_{\text{rev}}^{\varphi} = \min(\rho_{\text{rev}}^{\varphi_1}, \rho_{\text{rev}}^{\varphi_2}, \dots, \rho_{\text{rev}}^{\varphi_r})$. In this case, we first check whether the function φ_i is a predicate or not for all $i = 1, \dots, r$. If at least one function φ_i is not a predicate, we next replace $\rho_{\text{rev}}^{\varphi_i}$ with a variable. This step has to

²In the rest of this paper, the term *equivalent* when applied to two optimization problems means that the (global) optimal objective value and optimal solution (if they exist) of one problem can be obtained from those of the other, and vice versa. This is the same usage as in [28, p.257].

be considered differently depending on whether the outermost operator of $\rho_{\text{rev}}^{\varphi_i}$ is max or min, as will be explained in **(i. min-max)** and **(i. min-min)**, respectively.

(i. min-max) If the outermost operator of function $\rho_{\text{rev}}^{\varphi_i}$ ($i = 1, \dots, r$) is max, i.e., $\rho_{\text{rev}}^{\varphi_i} = \max(\rho_{\text{rev}}^{\varphi_1}, \dots, \rho_{\text{rev}}^{\varphi_y})$, we first replace $\rho_{\text{rev}}^{\varphi_i}$ with a variable s in $\rho_{\text{rev}}^{\varphi}$ as $\min(\rho_{\text{rev}}^{\varphi_1}, \dots, s, \dots, \rho_{\text{rev}}^{\varphi_r})$, then we add the following constraints:

$$\rho_{\text{rev}}^{\varphi_1} \leq s, \dots, \rho_{\text{rev}}^{\varphi_y} \leq s. \quad (11)$$

(i. min-min) On the other hand, if the outermost operator of the function $\rho_{\text{rev}}^{\varphi_i}$ ($i = 1, \dots, r$) is min, i.e., $\rho_{\text{rev}}^{\varphi_i} = \min(\rho_{\text{rev}}^{\varphi_1}, \dots, \rho_{\text{rev}}^{\varphi_y})$, we cannot apply the same transformation above. To replace $\rho_{\text{rev}}^{\varphi_i}$ with a variable s in $\rho_{\text{rev}}^{\varphi}$ as $\min(\rho_{\text{rev}}^{\varphi_1}, \dots, s, \dots, \rho_{\text{rev}}^{\varphi_r})$, we need to add non-convex constraints:

$$\min(\rho_{\text{rev}}^{\varphi_1}, \dots, \rho_{\text{rev}}^{\varphi_y}) = s. \quad (12)$$

(Part ii. from constraints to constraints) After these procedures, regardless of the outermost operator of the robustness function, either max or min, the robustness function in the objectives are now decomposed into the constraints in one of the three forms (12), (13), or (14):

$$\max(\rho_{\text{rev}}^{\Phi_1}, \dots, \rho_{\text{rev}}^{\Phi_{y_{\text{max}}}}) \leq s_{\text{max}}, \quad (13)$$

$$\min(\rho_{\text{rev}}^{\Psi_1}, \dots, \rho_{\text{rev}}^{\Psi_{y_{\text{min}}}}) \leq s_{\text{min}}, \quad (14)$$

where $s_{\text{min}}, s_{\text{max}}$ are variables and each function $\rho_{\text{rev}}^{\Phi_i}$ ($i = 1, \dots, y_{\text{max}}$), $\rho_{\text{rev}}^{\Psi_i}$ ($i = 1, \dots, y_{\text{min}}$) is a robustness function associated with subformulas Φ_i ($i = 1, \dots, y_{\text{max}}$) and Ψ_i ($i = 1, \dots, y_{\text{min}}$). These inequalities are paraphrased expressions of (10d) and (11) above. Note that these arguments of the max and min functions are still not necessarily predicates. We continue the following steps until all the arguments in each function become the predicates.

(ii. max) For inequality constraints of the form (13), we transform it as follows:

$$\rho_{\text{rev}}^{\Phi_1} \leq s_{\text{max}}, \rho_{\text{rev}}^{\Phi_2} \leq s_{\text{max}}, \dots, \rho_{\text{rev}}^{\Phi_{y_{\text{max}}}} \leq s_{\text{max}}. \quad (15)$$

This is of course equivalent with (13).

(ii. min) For constraints of the forms (12) or (14), we check whether each argument of the min of the left-hand side is a predicate or not, as the explanation of the case **(i. min)**. We then replace arguments that are not a predicate with variables depending on whether the outermost operators of those arguments are max or min, which will be described in **(ii. min-max)** and **(ii. min-min)** respectively. Each procedure is the same as **(i. min-max)** and **(i. min-min)** respectively except for one difference in the following **(ii. min-max)**.

(ii. min-max) If the outermost operator of the function $\rho_{\text{rev}}^{\Psi_i}$ ($i \in \{1, \dots, y_{\text{min}}\}$) is max, i.e., $\rho_{\text{rev}}^{\Psi_i} = \max(\rho_{\text{rev}}^{\psi_1}, \dots, \rho_{\text{rev}}^{\psi_v})$, we first replace function $\rho_{\text{rev}}^{\Psi_i}$ by a variable s_{new} as $\min(\rho_{\text{rev}}^{\psi_1}, \dots, s_{\text{new}}, \dots, \rho_{\text{rev}}^{\psi_{y_{\text{min}}}})$. Then, we add the following constraints:

$$\max(\rho_{\text{rev}}^{\psi_1}, \dots, \rho_{\text{rev}}^{\psi_v}) \leq s_{\text{new}}, \quad (16)$$

which is in the same form as (13).

(ii. min-min) If the outermost operator of the function $\rho_{\text{rev}}^{\Psi_i}$ ($i \in \{1, \dots, y_{\text{min}}\}$) is min, i.e., $\rho_{\text{rev}}^{\Psi_i} = \min(\rho_{\text{rev}}^{\psi_1}, \dots, \rho_{\text{rev}}^{\psi_v})$,

the procedure is same as **(i. min-min)**, which produce a new equality constraint of the form (12).

Subsequent to these procedures in **(Part ii.)**, constraints of the form (12), (13), or (14) are decomposed into constraints of one of these same forms. After we repeat this **(Part ii.)** again, these constraints are decomposed into the same forms. We repeat **(Part ii.)** until we reach the predicates, the bottom of the STL tree. This is the end of the procedure.

After this procedure, all concave constraints are in the forms of (12) or (14). The cost function is concave if and only if the outermost operator of the reversed robustness function is min. The other parts of the program are all convex.

C. Removing min-type equations by formula simplification

Although Procedure 1 remarkably makes the non-affine equality constraints fewer than the procedure described in the proof of Theorem 1, the reformulated program has still a considerable number of equality constraints of the form (12), which have to be approximated by CCP. To address this issue associated with the equations of the form (12), we additionally introduce an offline technique, called the simplification technique [8]. The simplification technique can unify (or remove) max and min functions in succession. This technique was first utilized in [8] for STL specifications to make integer variables fewer in the MIP-based formulation. However, we use this technique to remove the equations of the form (12) for our robustness decomposition. This can be easily explained through the tree structure of a robustness function: if there are two nodes whose type is the same (either max or min), then they can be unified into one node. Note that this unification is applied not only for boolean operators \vee, \wedge but also temporal operators $(\square, \diamond, \mathcal{U})$ as they are expressed as either max or min explained in Subsection III-A. We show an illustrative example of this simplification technique in Fig.2, where the simplified version of the robustness tree in Fig.1 is shown.

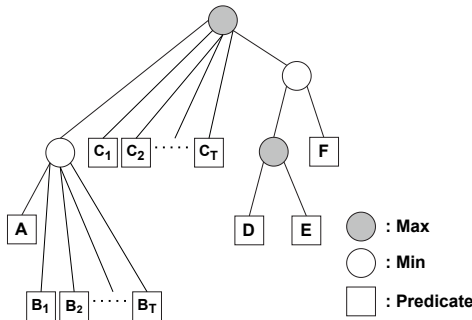


Fig. 2: The simplified version of the robustness tree in Fig.1.

We recursively simplify the tree from the top node to the bottom. If there may be more than two consecutive nodes that are the same type (e.g. min-min-min...), we repeat this simplification procedure (function SIMPLIFYONCE in Algorithm 4) until it does not have any consecutive same type nodes. As a result, the min-type equations (12) in **(i. min-min)** and **(ii. min-min)** can be removed by executing the simplification offline before the robustness decomposition, resulting in a

fewer approximation by CCP at each iteration. Moreover, this simplification brings us another benefit, i.e., it decreases the number of constraints. This is because the order of the constraints' number is proportional to that of nodes' number $\mathcal{O}(N_{p\wedge}^\varphi + N_V^\varphi)$ where N_V^φ decreases when we use the simplification technique. In the rest of this paper, formula φ indicates the simplified formula φ using this simplification technique offline. The overall reformulation procedure in Subsections IV-B and IV-C is summarized in Algorithm 1.

Algorithm 1 Program reformulation

Input: Original program (6)

Output: The reformulated program (**Cost, Constr**)

```

1: Simplify the formula (Algorithm 4);
2: Constr ← {(6b), (6c)}
3: if  $\rho_{\text{rev}}^\varphi = \max(\rho_{\text{rev}}^{\varphi_1}, \rho_{\text{rev}}^{\varphi_2}, \dots, \rho_{\text{rev}}^{\varphi_r})$  then
4:   Cost ← {(10a)};
5:   Constr ← Constr  $\cup$  {(10c), (10d)};
6: else (if  $\rho_{\text{rev}}^\varphi = \min(\rho_{\text{rev}}^{\varphi_1}, \rho_{\text{rev}}^{\varphi_2}, \dots, \rho_{\text{rev}}^{\varphi_r})$ )
7:   for each  $i \in \{1, \dots, r\}$  do
8:     if  $\rho_{\text{rev}}^{\varphi_i}$  is not a predicate then
9:       replace  $\rho_{\text{rev}}^{\varphi_i}$  in the arguments of  $\rho_{\text{rev}}^\varphi$  with a new
       variable  $s_i$ ;
10:    Constr ← Constr  $\cup$   $\{\max(\rho_{\text{rev}}^{\varphi_1}, \dots, \rho_{\text{rev}}^{\varphi_r}) \leq s\}$ ;
11:    Cost ← {(6a)};
12:    Constr ← Constr  $\cup$  {(6d)};
13: while  $\neg(\forall \text{constr} \in \text{Constr}, \text{every argument of the}$ 
    l.h.s of constr is either a predicate or a variable) do
14:   if constr is max form (13) then
15:     for each  $i \in \{1, \dots, y_{\text{max}}\}$  do
16:       if not all the arguments are predicates then
17:         Constr ← Constr  $-$  {(13)};
18:         Constr ← Constr  $\cup$  {(15)};
19:   if constr is min form (14) then
20:     for each  $i \in \{1, \dots, v\}$  in (14) do
21:       for each  $i \in \{1, \dots, y_{\text{min}}\}$  do
22:         Constr ← Constr  $-$  {(14)};
23:         Constr ← Constr  $\cup$   $\{\min(\rho_{\text{rev}}^{\varphi_1}, \dots, s_{\text{new}}, \dots, \rho_{\text{rev}}^{\varphi_{y_{\text{min}}}}) \leq s_{\text{min}}\}$ ;
24:         Constr ← Constr  $\cup$  {(16)};
```

D. The resulting program and its properties

If the outermost operator (top node) of the robustness function $\rho_{\text{rev}}^\varphi$ is max function, the resulting program \mathcal{P}_{DC} is written as follows.

$$\min_z s_\xi \quad (17a)$$

$$\text{s.t. (6b), (6c)} \quad (17b)$$

$$s_\xi \leq 0, \quad (17c)$$

$$\left. \begin{array}{l} \rho_{\text{rev}}^{\Phi_1^{(1)}} \leq s_{\text{max}}^{(1)}, \dots, \rho_{\text{rev}}^{\Phi_{y_{\text{max}}}^{(1)}} \leq s_{\text{max}}^{(1)} \\ \vdots \\ \rho_{\text{rev}}^{\Phi_1^{(v)}} \leq s_{\text{max}}^{(v)}, \dots, \rho_{\text{rev}}^{\Phi_{y_{\text{max}}}^{(v)}} \leq s_{\text{max}}^{(v)} \end{array} \right\} \text{from max nodes} \quad (17d)$$

$$\left. \begin{array}{l} \min(\rho_{\text{rev}}^{\Psi_1^{(1)}}, \dots, \rho_{\text{rev}}^{\Psi_{y_{\text{min}}}^{(1)}}) \leq s_{\text{min}}^{(1)} \\ \vdots \\ \min(\rho_{\text{rev}}^{\Psi_1^{(w)}}, \dots, \rho_{\text{rev}}^{\Psi_{y_{\text{min}}}^{(w)}}) \leq s_{\text{min}}^{(w)} \end{array} \right\} \text{from min nodes} \quad (17e)$$

where $\mathbf{z} = [\mathbf{x}^\top, \mathbf{u}^\top, s_\xi, s_{\max}^{(1)}, \dots, s_{\max}^{(v)}, s_{\min}^{(1)}, \dots, s_{\min}^{(w)}]^\top \in \mathbb{R}^{n+m+1+v+w}$ denotes the vector of optimization variables, where some slight abuse of notation is made such that some of the variables $s_{\max}^{(\cdot)}, s_{\min}^{(\cdot)}$ in constraints (17d),(17e) may represent s_ξ , and some of the arguments of the min functions (17e) are variables $s_{\max}^{(\cdot)}$. Note that all the robustness functions $\rho_{\text{rev}}^{(\cdot)}$ in this program are affine predicates and there are no max functions in this program anymore.

If the outermost operator is min, the resulting program is the same as the program (17), except that the cost function is a min function. However, it is worth noting that most of the specifications are of the max type, which is referred to as conjunction normal form (CNF) in [29], as specifications are typically written as a conjunction of sub-tasks such as reaching goals, avoiding obstacles, and so on. Moreover, the robustness simplification procedure does not change the type of the tree of \mathcal{T}^φ . Therefore, in the remainder of this paper, we concentrate on the STL formulas whose robustness tree \mathcal{T}^φ is max type for ease of explanation.

We now show that the reformulation by Algorithm 1 does not lose important properties of the original program (6) in the following two theorems. First, this transformation retains the soundness property.

Theorem 2: A feasible solution \mathbf{x} of the program \mathcal{P}_{DC} always satisfies the STL specification φ , i.e., $\mathbf{x} \models \varphi$.

Proof. From the equations (2) and (7), it is enough to show $\rho_{\text{rev}}^\varphi(\mathbf{x}') \leq 0$. This equation can be proved in the same way as the proof of [22, Proposition 1]. The only difference is whether we apply the Algorithm 1 for program \mathcal{P}_{DC} itself or its smoothed program, which does not affect the proof. \square

The following theorem states that the transformation is *equivalent* in our sense (see footnote 2).

Theorem 3: The program \mathcal{P}_{DC} is equivalent with (6).

Proof. This statement can be proved in the same way as the proof of [22, Theorem 1]. The only difference is whether we apply Algorithm 1 for program \mathcal{P}_{DC} itself or its smoothed program, which does not affect the proof. \square

By these two statements, this reformulation is guaranteed to retain the original properties. Moreover, by inspecting Procedure 1 from the tree perspective, we can see that those concave parts come only from *truly* disjunctive parts (17e) in \mathcal{P}_{DC} .

Proposition 1: Each concave constraint (17e) of the program \mathcal{P}_{DC} corresponds *one-to-one* with a disjunctive node in the simplified robustness tree.

Therefore, we can conclude that the concave parts are minimized and their curvature corresponds to the maximum curvature of each min function. As the convergence of the algorithm is faster in general when the curvature of the concave part is small [16, 17], this property is suitable for our framework.

V. SMOOTH APPROXIMATION BY MELLOWMIN

Another advantage of the resulting DC program \mathcal{P}_{DC} (17) is that smoothing only a small number of min functions in

(17e) makes the program differentiable as other functions are all differentiable. Although we can choose to solve the non-differentiable program (17) directly, this paper focuses on designing gradient-based algorithms. To this end, this section presents a novel min's smooth approximation that is suitable for our framework. Then, we define the corresponding robustness measure.

A. Alternative smooth approximation

In the literature [3, 4], the max and min functions in the robustness function (7) are smoothed by using the log-sum-exp (LSE) function, which we denote them as $\widetilde{\text{max}}_k := \frac{1}{k} \ln \sum_{i=1}^r e^{ka_i}$ and $\widetilde{\text{min}}_k := -\widetilde{\text{max}}_k(-\mathbf{a})$ respectively, where $k \in \mathbb{R}$ is the smooth parameter. Although this smooth function is differentiable everywhere, the resulting robustness is not sound (2) when we smooth the max and min functions of the robustness function with these $\widetilde{\text{max}}_k$ and $\widetilde{\text{min}}_k$ functions. This is a serious defect as a measure for guaranteeing safety. To make the smooth approximation sound, we have to smooth the min function with an over-approximation (note that we consider the reversed robustness $\rho_{\text{rev}}^\varphi$). With this in mind, we propose an alternative smooth function for the min function, which we call a mellowmin operator, expressed as follows.

Definition 5: (Mellowmin operator)

$$\widetilde{\text{min}}_k(\mathbf{a}) = -\text{mm}_k(-\mathbf{a}), \quad (18)$$

where $\mathbf{a} = [a_1, \dots, a_r]^\top$ and $\text{mm}_k(\mathbf{a}) = \frac{1}{k} \ln \left(\frac{1}{r} \sum_{i=1}^r e^{ka_i} \right)$ denotes the mellowmax function.

The mellowmax operator was proposed as an alternative softmax operator in reinforcement learning in [30] and can be thought of as a log-*average*-exp function, $\widetilde{\text{max}}_k$ which is an under-approximation of max function. Thus, $\widetilde{\text{min}}_k$ is an over-approximation of min.

Lemma 1: The mellowmin function $\widetilde{\text{min}}_k$ (18) is an over-approximation of the true min, and its error bound is given by:

$$0 \leq \widetilde{\text{min}}_k(\mathbf{a}) - \min(\mathbf{a}) \leq \frac{\log(r)}{k}. \quad (19)$$

Proof. See Appendix B. \square

B. Our new robustness

Now, we define a new robustness measure using the mellowmin function (18).

Definition 6: (Reversed mellowmin robustness) The reversed mellow robustness $\widetilde{\rho}_{\text{rev}}^{\varphi,k}(\mathbf{x})$ is defined by the quantitative semantics of (7) where every min function is replaced by the mellowmin operator $\widetilde{\text{min}}_k$ (18).

It is worth mentioning that our new robustness measure considers smooth approximation *only* for the min functions in the robustness as max functions are rather *decomposed*.

Theorem 4: (Soundness) For any trajectories \mathbf{x} and any STL specification φ , $\widetilde{\rho}_{\text{rev}}^{\varphi,k}(\mathbf{x})$ is sound, i.e.,

$$\widetilde{\rho}_{\text{rev}}^{\varphi,k}(\mathbf{x}) \leq 0 \implies \mathbf{x} \models \varphi. \quad (20)$$

Proof. See Appendix C. \square

Theorem 5: (Asymptotic completeness) For any trajectories \mathbf{x} and any STL specification φ , there exists a constant $k_{\min} (> 0)$ such that

$$|\rho_{\text{rev}}^{\varphi}(\mathbf{x}) - \widetilde{\rho}_{\text{rev}}^{\varphi,k}(\mathbf{x})| \leq \epsilon \text{ for all } k \geq k_{\min}. \quad (21)$$

Proof. See Appendix D. \square

This theorem ensures that the new robustness $\widetilde{\rho}_{\text{rev}}^{\varphi,k}(\mathbf{x})$ approaches the original robustness (1) as k approaches ∞ , meaning that this robustness asymptotically recovers the completeness property, i.e., $\widetilde{\rho}_{\text{rev}}^{\varphi,k}(\mathbf{x}) \geq 0 \implies \mathbf{x} \not\models \varphi$.

Using the smoothed min function above, we restate the program (22) by replacing the robustness (6a) with the new robustness in Definition 6:

$$\min_{\mathbf{x}, \mathbf{u}} \widetilde{\rho}_{\text{rev}}^{\varphi,k}(\mathbf{x}) \quad (22a)$$

$$\text{s.t. (6b), (6c)} \quad (22b)$$

$$\widetilde{\rho}_{\text{rev}}^{\varphi,k}(\mathbf{x}) \leq 0 \quad (22c)$$

Then, Algorithm 1 can transform this program into the program (17) such that min functions in (17e) are replaced by $\widetilde{\min}_k$ operators. Let us denote this smoothed program (22) as $\widetilde{\mathcal{P}}_{\text{DC}}$.

C. Advantages of using the mellowmin operator

As we can see in Theorems 4 and 5, the reversed mellow robustness function is sound and asymptotically complete. However, if our goal was to only satisfy these properties, the following soft-min operator $\widetilde{\min}_k := -\frac{\sum_{i=1}^r a_i e^{-ka_i}}{\sum_{i=1}^r e^{-ka_i}}$ could also be used [5]. However, this function $\widetilde{\min}_k$ is not appropriate for our algorithm as its curvature (convex or concave) depends on the parameter k and is undetermined. As discussed in Section IV, the curvature of functions must be acknowledged to use the CCP-based algorithm. In particular, if you use famous convex solvers such as CVXPY, this function won't be accepted. On the other hand, the curvature of the mellowmin is explicit:

Proposition 2: The mellowmin is concave for any $k > 0$.

Proof. From the the Hessian of mellowmax function $\widetilde{\max}$ in [35, p. 88], [36, Claim 1], the Hessian of the mellowmin is $\nabla^2 \widetilde{\min}_k = -\frac{k}{(\mathbf{1}^\top (-\boldsymbol{\sigma}))^2} ((\mathbf{1}^\top (-\boldsymbol{\sigma})) \text{diag}(-\boldsymbol{\sigma}) - (-\boldsymbol{\sigma})(-\boldsymbol{\sigma})^\top) \leq 0$. Thus, it is concave as long as $k \geq 0$. \square

Therefore, in the first place, the mellowmin $\widetilde{\min}_k$ is the only function that can retain the soundness (Theorem 4) while being usable for our algorithm among the possible smooth min functions including $\widetilde{\min}_k, \widehat{\min}_k$ (Proposition 2).

Moreover, the mellowmin function also has strict monotonicity with respect to each of its arguments for all values of the parameter $k > 0$ because $\frac{\partial \widetilde{\min}_k(\mathbf{a})}{\partial a_i} = -\frac{e^{-ka_i}}{\sum_{j=1}^r e^{-ka_j}} < 0$. This property is needed to prove the soundness and the equivalence of the reformulated program in the same way as the proof of Theorems 2 and 3.

Additionally, the following bound holds.

Proposition 3: the concaveness of the mellowmin operator is bounded by a value for a given k as

$$-k \|\mathbf{v}\|^2 \leq \mathbf{v}^\top \nabla^2 \widetilde{\min}_k(\mathbf{a}) \mathbf{v} \leq 0, \quad (23)$$

where $\mathbf{v} \in \mathbb{R}^r$ and $\|\mathbf{v}\|^2 = \mathbf{v}^\top \mathbf{v}$. This bound becomes tighter *monotonically* as $k \rightarrow 0$.

Proof. By taking minus signs on the bound on the Hessian of the mellowmax in [37], we have the equation (23). \square

From this proposition and Proposition 1, we can also see that the concaveness (bound) of the overall program $\widetilde{\mathcal{P}}_{\text{DC}}$ increases *monotonically* as $k \rightarrow \infty$. In other words, the program (22) gets closer to the original program (6) as $k \rightarrow \infty$ whereas it becomes a *convex* program as $k \rightarrow 0$.³ This property is useful in our framework as we can see the trade-off between the roughness of the majorization at each step and the completeness, which can be controlled by the parameter k . Due to these three reasons, the mellowmin function is the most suitable for CCP among the several possible functions.

VI. ITERATIVE OPTIMIZATION WITH PENALTY CCP

A. Properties of the subproblem

Under the general condition in Assumption 1, the subprogram after the majorization step described in Section II-B becomes a general convex program such as second-order cone programs (SOCP) and we have to solve them sequentially. However, thanks to the proposed decomposition, the subproblem can be an efficient form under certain conditions. Theorems 6 and 7 clarify these assumptions needed, i.e., Assumptions 2 and 3, respectively. Assumption 3 imposes a stronger condition on sets \mathcal{X}, \mathcal{U} and predicates of STL formula φ than Assumption 2.

Assumption 2: System (5) is linear, i.e., $x_{t+1} = Ax_t + Bu_t$, where $A \in \mathbb{R}^{n \times n}$ and $B \in \mathbb{R}^{n \times m}$. h_x, h_u of \mathcal{X}, \mathcal{U} , as well as the g^μ for all predicates μ of φ are all convex functions.

Assumption 3: System (5) is linear, i.e., $x_{t+1} = Ax_t + Bu_t$, where $A \in \mathbb{R}^{n \times n}$ and $B \in \mathbb{R}^{n \times m}$. h_x, h_u of \mathcal{X}, \mathcal{U} in (5), as well as the g^μ for all predicates μ of φ are also all composed of linear functions.

Theorem 6: Under Assumption 2, the parts of the program that we approximate in the majorization step of CCP are only inequalities in (17e).

Proof. The program \mathcal{P}_{DC} does not have nonaffine equality constraints as the one in Remark 2 when the only equation in (17) is linear. The program \mathcal{P}_{DC} is a convex program except for the concave constraints of the form (17e). From the explanations of CCP in Section II-B, the statement holds. \square

Theorem 7: Under Assumption 3, the program $\widetilde{\mathcal{P}}_{\text{DC}}$ after the majorization of CCP is a linear program (LP). If we add the quadratic cost function, the program can be written as a convex quadratic program (QP).

³This is because, if all min functions become average functions, the robustness becomes a convex function. The authors of [12] leverage this property to make the program a convex quadratic program. However, they had to restrict the range of STL specifications considerably. In this sense, our work can be seen as the extension of their work, where we allow all the STL specifications.

Proof. Similar to Theorem 6, the result follows by linearizing the concave constraints (17e) in the program \mathcal{P}_{DC} . \square

As a corollary of the above theorem, our CCP-based method is sequential linear programming. If we add the quadratic cost function in (22a), our method becomes sequential quadratic programming (SQP). These theorems are practically useful for analyzing the best setting for the proposed algorithm. In the subsequent discussions, we focus on the scenario in Assumption 3, where both properties outlined in Theorems 6 and 7 are valid. We denote the resulting subproblem under this assumption as \mathcal{P}_{LP} .

Furthermore, regardless of this computational efficiency above, the number of concave constraints (17e) is relatively small compared to the total number of constraints, as demonstrated by the following theorem and example.

Theorem 8: The number of constraints linearized at each iteration is proportional to the number of disjunctive nodes N_V^φ in the STL formulas, i.e., $\mathcal{O}(N_V^\varphi)$ whereas the number of all the constraints is proportional to the number of $N_{p\wedge}^\varphi$, N_V^φ , and T , i.e., $\mathcal{O}(N_{p\wedge}^\varphi + N_V^\varphi + T)$.

Proof. In (17), concave constraints are only of the form (17e). Proposition 1 states that these concave parts correspond to the disjunctive nodes of simplified robustness tree \mathcal{T}^φ . On the other hand, $\mathcal{O}(N_{p\wedge}^\varphi)$ comes from (17d), and $\mathcal{O}(T)$ comes from (17b). \square

Example 2: Consider the formula in Example 1 with $T = 20$. The number of concave constraints is 2, while the number of convex (including affine) constraints is 83, where 22 comes from equations in (17d), and 61 comes from equations in (17b) and (17c).

Furthermore, the feasible solution of the resulting program \mathcal{P}_{LP} also has soundness property.

Theorem 9: Let a decision variable vector $\mathbf{z} = [\mathbf{x}^\top, \dots]^\top$ be a feasible solution to the program \mathcal{P}_{LP} . The feasible trajectory \mathbf{x} always satisfies the STL specification φ , i.e., $\mathbf{x} \models \varphi$.

Proof. First, the first-order approximations of CCP at each step are global over-estimators; i.e., $f_i(\mathbf{z}) - g_i(\mathbf{z}) \leq f_i(\mathbf{z}) - g_i(\mathbf{z}_{(\cdot)}) + \nabla g_i(\mathbf{z}_{(\cdot)})^\top (\mathbf{z}_{(\cdot)} - \mathbf{z})$ where g_i is $z_{(\cdot)}$ is the current point of variable \mathbf{z} . Therefore, a feasible solution of the linear program \mathcal{P}_{LP} is a feasible solution to the program $\tilde{\mathcal{P}}_{DC}$. On the other hand, we can prove in the same way as Theorem 2 that a feasible solution of the program $\tilde{\mathcal{P}}_{DC}$ always satisfies $\tilde{\rho}_{\text{rev}}^{\varphi,k}(\mathbf{x}') \leq 0$. From this equation and Theorem 4, this feasible solution \mathbf{x} always satisfies the specification. Therefore, the statement holds. \square

B. Tree-weighted penalty CCP

In this subsection, we propose a heuristic extension of CCP, which we call the *tree-weighted penalty CCP (TWP-CCP)*, to improve the algorithm further by exploiting the *hierarchical* information of STL. Generally speaking, in an STL specification, each logical operator does not have the same importance. Using the words of the STL tree, nodes whose subtree has more leaves (predicates) are more essential than nodes whose

subtree has fewer leaves because the precision of the former has a higher influence on the overall tree than that of the latter.

To add this priority information into the algorithm, we follow the idea of *penalty CCP* [6], which introduced constraint relaxation to eliminate the need for an initial feasible point to initiate the algorithm. They relaxed the problem by adding variables to the constraints and penalizing the sum of the violations by adding them to the objective function. We extend this concept by exploiting Proposition 1, which demonstrates that in the resulting program, each constraint corresponds to an operator in the simplified STL specification individually. This characteristic allows us to penalize violations differently, thus enabling us to utilize the *priority* information of STL operators for optimization. This addresses a gap in previous literature where the priority ranking among nodes was overlooked due to the lack of a connection between constraints and STL nodes in the original formulation. We impose the priority weights on the penalty variable in each constraint where the weights are proportional to the number of leaves that the corresponding node has. **This priority information should be taken into account, particularly in the early stages of the optimization process. Otherwise, the violation of important constraints can happen in the early stages because of the problem relaxation of the penalty CCP, leading subsequent steps to go in the wrong direction.** For instance, the relaxed program of (3) is

$$\min_{\mathbf{z}} p_0(\mathbf{z}) + \tau_i \sum_{j=1}^m N^{\varphi_j} s_j \quad (24a)$$

$$\text{s.t. } p_j(\mathbf{z}) \leq s_j, \quad j = \{1, \dots, m\} \quad (24b)$$

$$s_j \geq 0, \quad j = \{1, \dots, m\}. \quad (24c)$$

The TWP-CCP procedure is summarized in Algorithm 2, where $z_{(i)}$ denotes the current value at each iteration. The meaning of other symbols is the same as Subsection II-B.

Algorithm 2 Tree-Weighted Penalty CCP

Input: Parameters: an initial point z_0 , an initial weight $\tau_0 > 0$ and its maximum constant $\tau_{\max} > 0$ and its rate of change at each iteration, $\mu > 1$, and a stopping criterion.

- 1: Compute the number of leaves N^{φ_j} associated with each constraint for $j = 1, \dots, m$, and initialize: $i := 0$;
 - 2: Majorize the concave terms $g_j, j = 0, \dots, m$ in (24) to $\hat{g}_j(\mathbf{z}) = g_j(z_{(i)}) + \nabla g_j(z_{(i)})^\top (\mathbf{z} - z_{(i)})$ and solve the convex program;
 - 3: Update $\tau_{i+1} := \min(\mu\tau_i, \tau_{\max})$;
 - 4: Update iteration as $i := i + 1$. Repeat until the stopping criterion is satisfied;
-

The solution of program \mathcal{P}_{LP} satisfies the STL specification in the limit of the penalty variables $s_j \rightarrow 0$ for $j \in \{1, \dots, m\}$ ($\tau_i \rightarrow \infty$) because the program (24) reduces to program \mathcal{P}_{LP} . This holds in practice, as the penalty variables take a value close to 0 if it converges. The overall framework *STLCCP* is summarized in Algorithm 3.

VII. NUMERICAL SIMULATIONS

In this section, we demonstrate the effectiveness of our proposed method over state-of-the-art methods through four

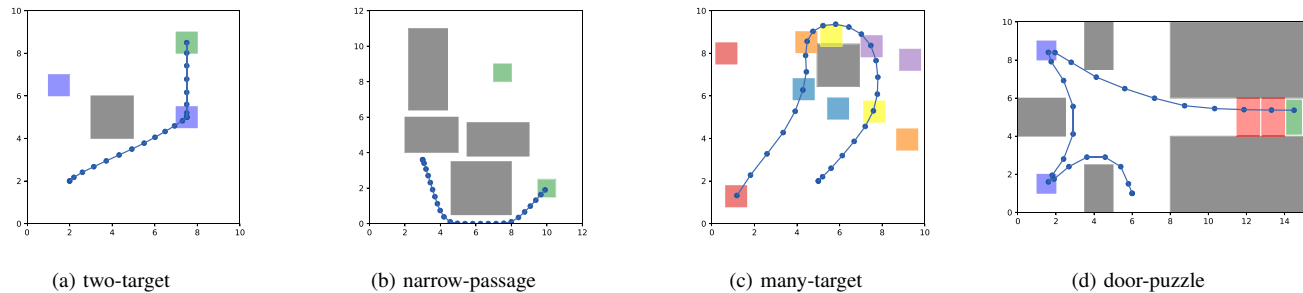


Fig. 3: Illustrations of scenarios along with solutions generated by MIP-based method with $T = 25$.

Algorithm 3 STLCCP

- 1: Transform Problem 1 to (22) by applying new smooth robustness in Definition 6 (Sections II and V);
 - 2: Reformulate (22) into $\tilde{\mathcal{P}}_{\text{DC}}$ (e.g. (17)) by Algorithm 1 (Section IV);
 - 3: Optimize via tree-weighted penalty CCP by Algorithm 2 (Section VI);
-

benchmark scenarios. During the experiment in Subsection VII-F, we also propose a practical remedy, the warm-start approach, to effectively utilize the mellowmin functions. All experiments were conducted on a MacBook Air 2020 with an Apple M1 processor (Maximum CPU clock rate: 3.2 GHz) and 8GB of RAM. Note that in this section, all robustness scores refer to the scores calculated from the original robustness semantics (1).

A. Compared methods

Proposed approach: We implemented our algorithm in Python using CVXPY [31] as the interface to the optimizer. As for the smooth min function for reversed robustness function, the first three experiments in VII-C–VII-E focus on the LSE smoothing ($k = 10$) in [22, Definition 2] to show the validity of our reformulation method, whereas the final subsection shows the effectiveness of the mellowmin smoothing ($k = 1000$) in Definition 6. For the solving step, we used the QP-solver of GUROBI (ver. 10) [32] with the default option (parallel barrier algorithm). Unless otherwise noted, we took the TWP-CCP described in Subsection II-B to solve the reformulated program. The penalty variables were introduced only for the concave constraints. This is because CCP only approximates such concave parts and there is less need to admit the violation for the convex parts. We employed a normal distribution to vary the initial values of variables in each sample. If the optimization failed to converge within 25 iterations, we regarded our method as unsuccessful and terminated the optimization. However, in most of the problems we solved, the terminal condition was met within 15 iterations. All the parameters for the CCP shown in Table II are fixed throughout this paper.

The compared two methods are summarized as follows. They are one of the most popular and fastest methods in MIP-based and the SQP-based method, respectively.

TABLE II: Parameters for CCP.

Parameters	Description	Value
τ	initial weight on penalty variables in the cost	5e-3
μ	rate at which τ increases	2.0
$\tau_{\max, \mu}$	maximum τ	1e3
s_{terminal}	maximum values of penalty variables for terminal condition	1e-5
ep	maximum cost difference for terminal condition	1e-2
r	rate of exponential decay (only for Subsection VII-E)	0.2

MIP-based approach: GUROBI-MIP For the MIP-based approach, we formulated the problem as a MIP one using the encoding framework in [33] and solved the problem with the GUROBI solver, which we call GUROBI-MIP method. Note that GUROBI is often the fastest MIP solver.

SQP-based approach: SNOPT-NLP The SQP-based method we employed is based on the naive sequential quadratic programming (SQP) approach using the smoothing method proposed in [5] where they combine smoothing method using LSE and Boltzman softmax. Among the various SQP-based solvers available, we chose the SNOPT sparse SQP solver [34] because it is considered to be one of the best solvers for STL specifications among the SQP approaches, which outperforms Scipy’s SQP solver (similar arguments can be found in [5, 8]). All the parameter options of the SNOPT-NLP method were left at their default settings. We refer to this method as the SNOPT-NLP method.

B. Systems and specifications

Note that the state \mathbf{x} and input \mathbf{u} are defined as $\mathbf{x} = [p_x, p_y, \dot{p}_x, \dot{p}_y]^\top$ $\mathbf{u} = [\ddot{p}_x, \ddot{p}_y]^\top$, where p_x is the horizontal position of the robot and p_y is the vertical position. As for the system dynamics, we use a double integrator, i.e., a system (5) with the matrices $A = \begin{bmatrix} I_2 & I_2 \\ 0_{2 \times 2} & I_2 \end{bmatrix}$, $B = \begin{bmatrix} 0_{2 \times 2} \\ I_2 \end{bmatrix}$.

All four benchmark scenarios were borrowed from [8], which are standard scenarios involving a robot exploring a planar environment. The illustration of all four scenarios is shown in Figures 3c, with the solution obtained by MIP based method with $T = 25$. In this picture, the greyed regions express obstacles (O) that the robot must avoid for all time steps. The green regions express goals (G) that the robot must reach at the last time step. Other regions colored purple,

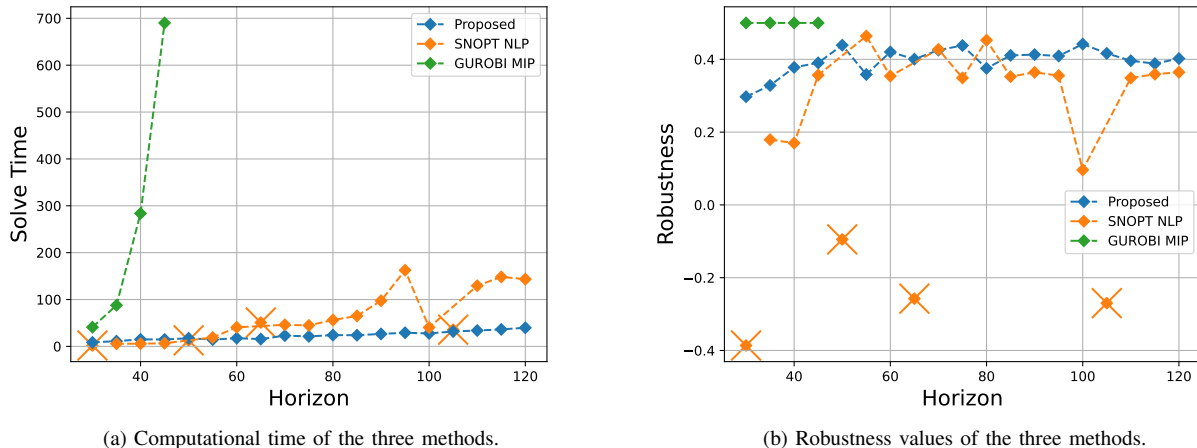


Fig. 4: Computational time and robustness score of the three methods in the many-target scenario over Horizon from $T = 30$ to 120.

blue and orange, and pink represent areas that the robot must pass through (or stop by) at least one-time step. For the specification of two-target and narrow-passage, the robot must pass through one of the two same color regions, while in the many-target specification, the robot must reach both two same color regions. In the door-puzzle specification, the robot has to collect keys (K) in the two blue regions to open the corresponding doors represented by the red and green regions in the figure. Specifically, the STL specification for each scenario is expressed as the following four formulas.

two-target:

$$\diamond_{[0, T-5]} (\square_{[0, 5]} T_1 \vee \square_{[0, 5]} T_2) \wedge \square_{[0, T]} \neg O \wedge \diamond_{[0, T]} G \quad (25a)$$

narrow-passage:

$$\diamond_{[0, T]} (G_1 \vee G_2) \wedge \square_{[0, T]} \left(\bigwedge_{i=1}^4 \neg O_i \right) \quad (25b)$$

many-target:

$$\bigwedge_{i=1}^5 \left(\bigvee_{j=1}^2 \diamond_{[0, T]} T_i^j \right) \wedge \square_{[0, T]} (\neg O), \quad (25c)$$

door-puzzle:

$$\bigwedge_{i=1}^2 (\neg D_i \mathbf{U}_{[0, T]} K_i) \wedge \diamond_{[0, T]} G \wedge \square_{[0, T]} \left(\bigwedge_{i=1}^5 \neg O_i \right). \quad (25d)$$

We would like to insist that the robot is not given the value of the initial speed in all the scenarios. Let us choose a specification from equations of (25) and express it as φ . We provide four sets of experimental results, each corresponding to each subsection.

Remark 5: (Small quadratic cost) To show our framework is effective in practical situations, we introduced a quadratic cost function $w_q \sum_{t=0}^T (x_t^T Q x_t + u_t^T R u_t)$, where Q and R are positive semidefinite symmetric matrices and w_q is a weight parameter. The value of w_q was set to 0.01 or 0.001.

Remark 6: (A modification for the SNOPT-NLP) In almost all the scenarios, the SNOPT-NLP solver returns the infeasible error message for Problem 1 with the robustness constraint (6d). To make the comparison more meaningful, we removed

the robustness constraint only for the SNOPT-NLP method, which makes the problem easier to solve.

C. Comparison over different horizons

As the first experiment, we evaluated the performance of our proposed method against the SQP-based method and the MIP-based method on a specific scenario, that is, the many-target specification (25c), with varying time horizons ranging from $T = 30$ to 120. The results are presented in Fig. 4, which compares the computation time of the three methods in Fig. 4a and their corresponding robustness scores in Fig. 4b. Note that in Fig. 4b, the SNOPT-NLP method sometimes takes negative values as we omit the robustness constraint (6d) for this method (see Remark 6). The orange \times marker in Fig. 4a shows the SNOPT-NLP's failure at the corresponding time horizon, meaning that the SNOPT-NLP method is stuck to local solutions with robustness less than or equal to 0, as shown in Fig. 4a. The blue plots in these figures are representing the average values of 5 trials of the proposed method as these results significantly depend on the initial value of variables. We omit the box plot of the variance for the sake of visibility (the variance is plotted in the box plot of Fig. 6). In the case of the other two methods, on the other hand, the results do not change by trial.

The computation time of the MIP-based method increases significantly as the horizon increases. The comparison of the two SQP-based methods shows that our proposed method was able to find satisfactory trajectories for all horizons within the given range of horizons, whereas the SQP-based method failed to find solutions on four horizons of $T = 30, 50, 65,$ and 105 (marked by the orange \times). It is worth noting that the robustness scores of our proposed method were consistently higher than 0, not only in the average of 5 samples but also in each of the five samples. This means that our method was successful in 95 out of 95 (19×5) experiments (100.00%). On the other hand, the SNOPT-NLP method succeeds in 15 out of 19 samples (78.95%) even though the robustness constraint (22c) is turned off.

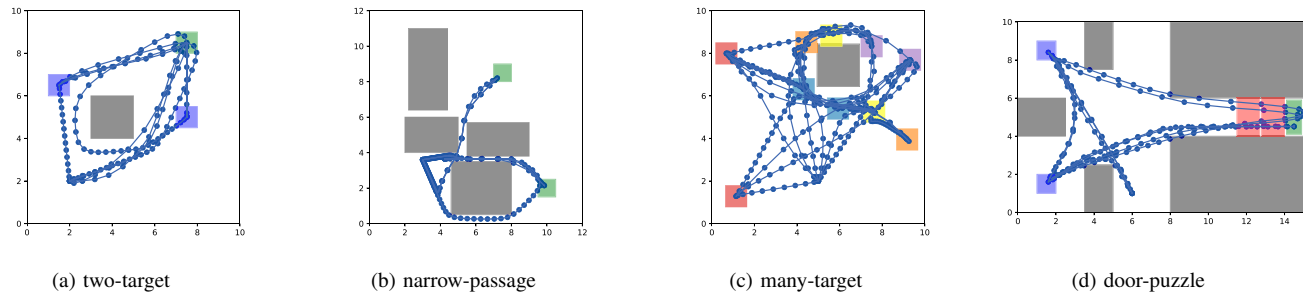


Fig. 5: Illustrations of scenarios along with the satisfactory trajectories generated by the proposed method with $T = 50$. Our method produced a range of satisfactory trajectories, each dependent on the initial guesses.

TABLE III: Solve times and robustness scores for the four different scenarios. Each value for our method represents the average of successful trials out of 10. If the robustness score for the SNOPT-NLP method is negative, it is labeled as “Failed”. If the solve time for GUROBI-MIP exceeds the allotted time of 7500, it is labeled as “Time out”.

Scenario	Horizon (T)	Solve Time (s)			Robustness			Success Rate		
		Ours	SNOPT-NLP	MIP	Ours	SNOPT-NLP	MIP	Ours	SNOPT-NLP	MIP
two-target	50	23.13	15.28	15.08	0.494	0.367	0.500	80.0 %	100.0 %	100.0 %
	75	26.76	Failed	193.82	0.500	Failed	0.500	90.0 %	Failed	100.0 %
	100	37.19	57.24	337.31	0.500	0.462	0.500	100.0 %	100.0 %	100.0 %
many-target	50	16.19	Failed	2526.99	0.440	Failed	0.500	100.0 %	Failed	100.0 %
	75	21.45	44.78	>7500.00	0.430	0.349	Time Out	100.0 %	100.0 %	Time Out
	100	27.80	40.39	>7500.00	0.437	0.096	Time Out	100.0 %	100.0 %	Time Out
narrow-passage	50	22.21	Failed	36.74	0.151	Failed	0.400	100.0 %	Failed	100.0 %
	75	35.18	8.83	>7500.00	0.027	0.151	Time Out	80.0 %	100.0 %	Time Out
	100	57.41	39.94	>7500.00	0.111	0.170	Time Out	100.0 %	100.0 %	Time Out
door-puzzle	50	299.33	Failed	>7500.00	0.348	Failed	Time Out	30.0 %	Failed	Time Out
	75	Failed	Failed	>7500.00	Failed	Failed	Time Out	< 5.0 %	Failed	Time Out
	100	Failed	Failed	>7500.00	Failed	Failed	Time Out	< 5.0 %	Failed	Time Out

Moreover, the convergence time of our proposed method only increases *slightly* as the horizon increases. In contrast, the SNOPT-NLP method experiences significant fluctuations in its performance as the horizon gets larger, and it takes longer to converge than our proposed method for all horizons $T \geq 55$, with a poorer robustness value in most cases. It’s worth noting that while the computation time of the SNOPT-NLP method may appear to decrease at horizons $T = 100, 105$, this is due to either a failure ($T = 105$) or a low robustness value of approximately 0.1 ($T = 100$), as shown in Fig. 4b, indicating that the optimization process is getting stuck in a local solution at an early stage of the optimization. Fig. 4b also demonstrates that our proposed method consistently takes a higher robustness score than the SNOPT-NLP method, achieving an average score of around 0.4, which is close to the global optimum 0.5 obtained by the MIP-based method. In contrast, the SNOPT-NLP method outputs a failure trajectory with a negative robustness value in some horizons.

Our method’s superiority in this scenario can be attributed to the fact that the number of concave constraints (17e), i.e., 81, is significantly less than the total number of constraints in (17), i.e., 3579 (including all the constraints in (17b)–(17e)).

D. Comparison over different specifications

Our next experiment compared the performance of three methods across four different scenarios, namely the two-target, narrow-passage, many-target, and door-puzzle scenarios. Table III presents the convergence times, the robustness scores, and the success rate of the three methods. They essentially show that only our method can output satisfactory trajectories

for all the horizons of the two-target, many-target, and narrow-passage scenarios. Moreover, our method significantly outperforms the other methods in both the two-target and many-target specifications. Furthermore, Only our method is able to synthesize a satisfactory trajectory for the door-puzzle scenario with $T = 50$.

It should be noted that the success rate of our method was above 90% in the two-target (27/30) and narrow-passage scenarios (28/30) and 100% in the many-target scenario (30/30), meaning that our method is robust against the initial guesses of variables, whereas, in the door-puzzle scenario, it was 30% (3/10). However, this is remarkable because these difficult scenarios over horizons were thought to be difficult to solve. Although our method also sometimes succeeded in $T = 75$ and $T = 100$, we did not list the details of these cases as their success rates were low.

Regarding the computational time, our proposed method is the fastest in the majority of the horizons in two-target and many-target scenarios. whereas the SNOPT-NLP sometimes does better than our approach in the narrow-passage scenario. Moreover, our method’s convergence time only increases slightly even when the horizon becomes longer, which is consistent with our observations in Subsection VII-C. Regarding the robustness score, our proposed method consistently produces a range of satisfactory trajectories while the SNOPT-NLP method exhibits a high degree of volatility, with a tendency to fail randomly in certain scenarios. For example, it produced a robustness score of 0.462 out of 0.500 in the two-target specifications with $T = 100$, but failed the same specification with $T = 75$ with a score of -0.506 . On the other

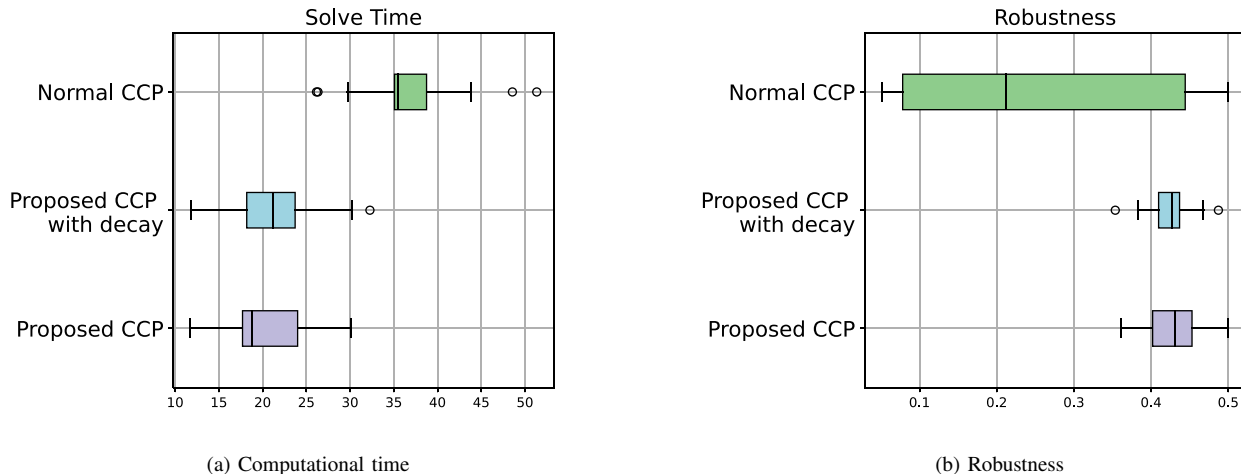


Fig. 6: Box plots of 20 samples for each method for the many-target scenario with $T = 75$.

hand, each trial of our method has a success rate of almost 100%, not only the averages of 10 trials given different initial values. These results demonstrate that our proposed method is robust against the values of initial guesses.

The relatively poorer performance of our method in the narrow-passage scenario likely stems from a combination of two factors: the narrowness of the path and the problem relaxation by penalty variables (not the iterative linearization itself). Our linearization targets only the constraints coming from the goal specification $\diamond_{[0,T]}(G_1 \vee G_2)$ (with a disjunctive node that unifies $\diamond_{[0,T]}$ and \vee). It does not linearize those from the obstacle avoidance $\square_{[0,T]}(\bigwedge_{i=1}^4 \neg O_i)$, as it does not have disjunctive nodes. Since linearizing the goal specification doesn't significantly worsen the challenges posed by the narrow path, it's unlikely the primary issue. (This is also supported by the strong performance of our method in the many-target scenario, which involves even more disjunctive goal nodes). However, our relaxation approach, combined with obstacle avoidance, does slow down the process. Our method initially allows for relatively large penalty variables, resulting in trajectories that may violate specifications (e.g., passing through the center of obstacles). We then gradually reduce these violations by increasing the weight of penalty variables. Guided by the robustness function, the trajectory iteratively converges to the narrow path (i.e., the feasible region). However, this process increases computational time and decreases robustness scores. These performances could be improved by adjusting parameters. For example, increasing the weighting on penalty variables would lead to faster convergence to the feasible region, and tightening terminal conditions would boost the final robustness score. While we did not extensively explore optimal parameter settings in this paper to ensure a fair comparison between methods, this remains an interesting area for future investigation.

Fig. 5a–5d displays several final trajectories generated by our proposed method with different initial values for all scenarios with $T = 50$. These figures illustrate that our method is flexible enough to find a solution that satisfies the

specifications regardless of the initial values.

E. Effectiveness of the tree weighted penalty CCP

In the third experiment, we compare the proposed tree-weighted penalty CCP (TWP-CCP) with the standard penalty CCP, referred to as a normal CCP, to show that the TWP-CCP improves the robustness score and convergence time. In this normal CCP, all the penalty weights N^{φ_j} of the concave constraints $i \in I$ are equal to the smallest number of child nodes each node has.

To make the comparison more persuasive, we also consider a variant of tree-weighted penalty CCP, which we call a proposed CCP *with decay*, as a comparison method. This method can be considered an intermediary approach between the proposed CCP and the normal CCP. Specifically, the penalty weight for each constraint j is chosen as

$$\sum_{j=1}^m (N^{\varphi_j} - \min_{j \in J} (N^{\varphi_j}) \exp(-r_p(i-1)) + \min_{j \in J} (N^{\varphi_j})) \tau s_j,$$

where i is the current iteration number, N^{φ_j} is the tree weight for constraint j , and s_j is the sum of all the variables of each concave constraint, r_p is the parameter that adjusts the exponential decay rate. $\min_{j \in J} (N^{\varphi_j})$ is the lowest number of the tree weight constant. This method initially starts as a proposed CCP, which gives priority ranking to the constraints according to the robustness tree, but then it exponentially approaches the normal CCP.

We evaluate the performance of three different methods in the many-target scenario with horizon $T = 75$. The robustness scores and convergence times for each method are illustrated in Figs. 6b and 6a, respectively, using box plots. Each box plot represents the results from 20 samples, which were generated by randomly varying the initial values of the variables.

Fig. 6b shows that the two TWP-CCP methods output much higher robustness scores than the normal CCP, and their convergence times are also lower on average. The results of the proposed method with decay, which only puts tree weight at early iterations, are comparable to the proposed method in Fig. 6b and Fig. 6a. This result suggests a hypothesis that it

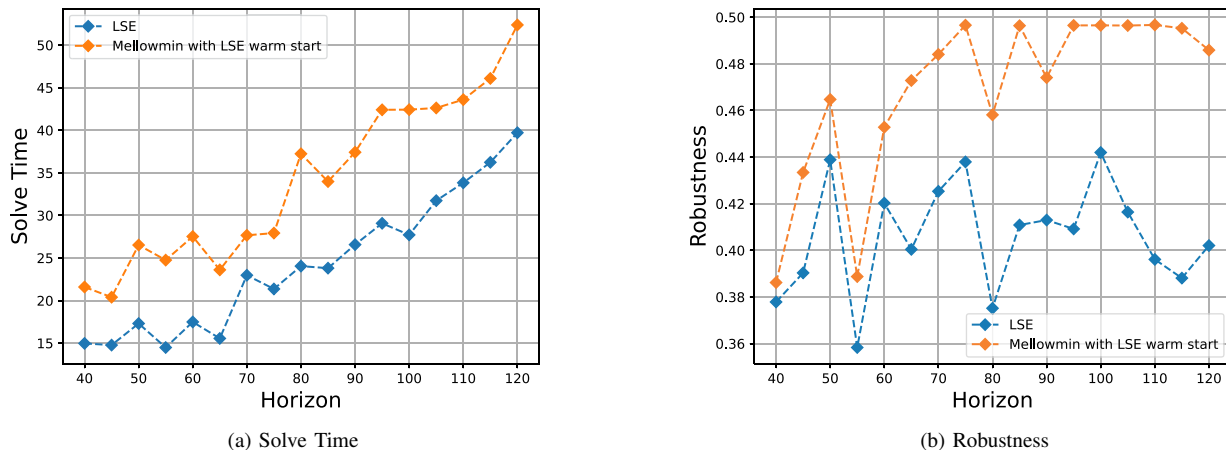


Fig. 7: Computational time and robustness score of the two methods in the many-target scenario over Horizon from $T = 40$ to 120. The orange plot additionally solves the mellowmin smoothed program $\tilde{\mathcal{P}}_{DC}$ using the solution of the blue plots.

is essential to incorporate the priority ranking, particularly in the early steps of the optimization process. This hypothesis was also verified when we analyzed how the value of each variable changes during the optimization of the normal CCP. Our experiment shows that when the normal CCP failed to find a satisfactory trajectory, the reason for this failure is, in most cases, high values of variables attached to the important constraints. As they weigh all constraints as equally important, they can easily neglect to observe those constraints, which can lead the optimization process to a local optimum.

F. Effectiveness of the mellowmin smoothing

In all experiments in Subsections VII-C–VII-E, we adopted LSE smoothing with $k = 10$ to demonstrate the effectiveness of our basic idea. However, the LSE smoothing approach does not have the same desirable properties as the mellowmin smoothing approach, such as the soundness property as described in Subsection V-C. However, we observed that purely solving the mellowmin smoothed program alone often results in a poor solution. This is likely because the smooth parameter k of mellowmin must be set high (e.g. 1000) to approximate the true min function accurately. This high value of k makes the function more likely to be affected by only one argument with the critical value, similar to the true min function, resulting in the transformed program being more prone to getting stuck in a local minimum. Therefore, we propose using the solution obtained from LSE smoothing as a warm start for the mellowmin smoothed program. The following two sets of experimental results demonstrate that this approach brings us a higher robustness score while maintaining theoretical guarantees such as soundness.

Fig. 7 compares the LSE smoothing and mellowmin smoothing using the LSE solution as a warm start in the many-target specification. The difference between the two plots in Fig. 7a represents the time required to solve the mellowmin smoothed program as the additional step. We observed that both approaches effectively find a solution with the fixed parameter $k = 10$ and 1000, respectively. In particular, it is

worth noting that the mellowmin smoothing approach always finds a solution although it is possible that $\tilde{\mathcal{P}}_{DC}$ does not find any solution even when the original problem \mathcal{P}_{DC} has one⁴. The robustness score becomes higher than when solely using the LSE function, which sometimes achieves the global optimum 0.5. Additionally, the average computational time to solve the mellowmin smoothed program remains low, around 10 seconds, even as the planning horizon increases. This is likely because a solution from the LSE smoothed program is already a good trajectory. The resulting solution of the warm start approach is always guaranteed to be sound, i.e., $x \models \varphi$.

We have also validated the effectiveness of this warm-start approach in the door-puzzle scenario. By repeating the warm-started mellowmin approach, we observed an increase in the success rate from 30.0% to 40.0% (for further details, please refer to the data provided in the GitHub link).

VIII. CONCLUSION

In this study, we established a connection between STL and CCP, and used it to propose an efficient optimization framework. Our novel structure-aware decomposition of STL formulas enabled us to encode the control problem into an efficient DC program, where only the concave constraints corresponding to the disjunctive nodes of the STL tree were linearized. To further enhance the efficiency and formality of our algorithm, we introduced a new smoothing function, called the mellowmin function, and an extension of CCP, called TWP-CCP. Both of these enhancements were shown to be effective in our experiments. Future work will explore extending our framework to problems beyond static synthesis, including those involving time delays and real-time uncertainties.

REFERENCES

- [1] O. Maler and D. Nickovic, “Monitoring temporal properties of continuous signals,” in *Formal Techniques, Modelling and Analysis of Timed and Fault-Tolerant Systems*, 2004, pp. 152–166.

⁴In such cases, you can either increase the value of k , use a different initial state, or repeat the warm-started mellowmin approach to solve the problem.

- [2] G. E. Fainekos and G. J. Pappas, “Robustness of temporal logic specifications for continuous-time signals,” *Theoretical Computer Science*, vol. 410, no. 42, pp. 4262–4291, 2009.
- [3] Y. V. Pant, H. Abbas, and R. Mangharam, “Smooth operator: Control using the smooth robustness of temporal logic,” in *IEEE Conference on Control Technology and Applications (CCTA)*, 2017, pp. 1235–1240.
- [4] W. Hashimoto, K. Hashimoto, and S. Takai, “STL2vec: Signal temporal logic embeddings for control synthesis with recurrent neural networks,” *IEEE Robotics and Automation Letters*, vol. 7, no. 2, pp. 5246–5253, 2022.
- [5] Y. Gilpin, V. Kurtz, and H. Lin, “A smooth robustness measure of signal temporal logic for symbolic control,” *IEEE Control Systems Letters*, vol. 5, no. 1, pp. 241–246, 2021.
- [6] T. Lipp and S. Boyd, “Variations and extension of the convex–concave procedure,” *Optimization and Engineering*, vol. 17, no. 2, pp. 263–287, 2016.
- [7] X. Shen, S. Diamond, Y. Gu, and S. Boyd, “Disciplined convex–concave programming,” in *IEEE Conference on Decision and Control (CDC)*, 2016, pp. 1009–1014.
- [8] V. Kurtz and H. Lin, “Mixed-integer programming for signal temporal logic with fewer binary variables,” *IEEE Control Systems Letters*, vol. 6, pp. 2635–2640, 2022. Their source code is available at <https://stlpy.readthedocs.io>.
- [9] S. Karaman and E. Frazzoli, “Vehicle routing problem with metric temporal logic specifications,” in *IEEE Conference on Decision and Control (CDC)*, 2008, pp. 3953–3958.
- [10] S. Karaman, R. G. Sanfelice, and E. Frazzoli, “Optimal control of mixed logical dynamical systems with linear temporal logic specifications,” in *IEEE Conference on Decision and Control (CDC)*, 2008, pp. 2117–2122.
- [11] V. Raman, A. Donzé, M. Maasoumy, R. M. Murray, A. Sangiovanni-Vincentelli, and S. A. Seshia, “Model predictive control with signal temporal logic specifications,” in *IEEE Conference on Decision and Control (CDC)*, 2014, pp. 81–87.
- [12] L. Lindemann and D. V. Dimarogonas, “Robust control for signal temporal logic specifications using discrete average space robustness,” *Automatica*, vol. 101, pp. 377–387, 2019.
- [13] N. Mehdipour, C. I. Vasile, and C. Belta, “Specifying user preferences using weighted signal temporal logic,” *IEEE Control Systems Letters*, vol. 5, no. 6, pp. 2006–2011, 2021.
- [14] I. Haghghi, N. Mehdipour, E. Bartocci, and C. Belta, “Control from signal temporal logic specifications with smooth cumulative quantitative semantics,” in *IEEE Conference on Decision and Control (CDC)*, 2019, pp. 4361–4366.
- [15] D. Sun, J. Chen, S. Mitra, and C. Fan, “Multi-agent motion planning from signal temporal logic specifications,” *IEEE Robotics and Automation Letters*, 2022.
- [16] F. Debrouwere, W. Van Loock, G. Pipeleers, Q. T. Dinh, M. Diehl, J. De Schutter, and J. Swevers, “Time-optimal path following for robots with convex–concave constraints using sequential convex programming,” *IEEE Transactions on Robotics*, vol. 29, no. 6, pp. 1485–1495, 2013.
- [17] Q. Tran Dinh, S. Gumussoy, W. Michiels, and M. Diehl, “Combining convex–concave decompositions and linearization approaches for solving BMIs, with application to static output feedback,” *IEEE Transactions on Automatic Control*, vol. 57, no. 6, pp. 1377–1390, 2012.
- [18] M. Cubuktepe, N. Jansen, S. Junges, J.-P. Katoen, and U. Topcu, “Convex optimization for parameter synthesis in MDPs,” *IEEE Transactions on Automatic Control*, vol. 67, pp. 6333–6348, 2021.
- [19] Q. Wang, M. Chen, B. Xue, N. Zhan, and J.-P. Katoen, “Encoding inductive invariants as barrier certificates: Synthesis via difference-of-convex programming,” *Information and Computation*, vol. 289, p. 104965, 2022.
- [20] M. Charitidou and D. V. Dimarogonas, “Signal temporal logic task decomposition via convex optimization,” *IEEE Control Systems Letters*, vol. 6, pp. 1238–1243, 2022.
- [21] Y. Mao, B. Acikmese, P.-L. Garoche, and A. Chapoutot, “Successive convexification for optimal control with signal temporal logic specifications,” in *ACM International Conference on Hybrid Systems: Computation and Control (HSCC)*, 2022, pp. 1–7.
- [22] Y. Takayama, K. Hashimoto, and T. Ohtsuka, “Signal temporal logic meets convex–concave programming: A structure-exploiting SQP algorithm for STL specifications,” in *IEEE Conference on Decision and Control (CDC)*, 2023, pp. 6855–6862.
- [23] S. Sadraddini and C. Belta, “Formal synthesis of control strategies for positive monotone systems,” *IEEE Transactions on Automatic Control*, vol. 64, no. 2, pp. 480–495, 2019.
- [24] —, “Robust temporal logic model predictive control,” in *Annual Allerton Conference on Communication, Control, and Computing (Allerton)*, pp. 772–779, 2015.
- [25] C. Baier and J.-P. Katoen, *Principles of Model Checking*. MIT Press, 2008.
- [26] K. Leung, N. Aréchiga, and M. Pavone, “Backpropagation for parametric STL,” in *IEEE Intelligent Vehicles Symposium (IV)*, pp. 185–192, 2019.
- [27] B. K. Sriperumbudur and G. R. G. Lanckriet, “On the convergence of the concave–convex procedure,” in *Advances in Neural Information Processing Systems (NIPS)*, vol. 22, 2009.
- [28] G. C. Calafiore and L. El Ghaoui, *Optimization Models*. Cambridge University Press, 2014.
- [29] S. Sadraddini, J. Rudan, and C. Belta, “Formal synthesis of distributed optimal traffic control policies,” in *8th International Conference on Cyber-Physical Systems (ICCPs)*, p. 15–24, 2017.
- [30] K. Asadi and M. L. Littman, “An alternative softmax operator for reinforcement learning,” in *International Conference on Machine Learning (ICML)*, vol. 70, pp. 243–252, 2017.
- [31] S. Diamond and S. Boyd, “CVXPY: A Python-Embedded modeling language for convex optimization,” *Journal of Machine Learning Research*, vol. 17, 2016.
- [32] Gurobi Optimization, LLC, “Gurobi Optimizer Reference Manual,” 2023. [Online]. Available: <https://www.gurobi.com>
- [33] C. Belta and S. Sadraddini, “Formal methods for control synthesis: An optimization perspective,” *Annual Review of Control, Robotics, and Autonomous Systems*, vol. 2, no. 1, pp. 115–140, 2019.
- [34] P. E. Gill, W. Murray, and M. A. Saunders, “SNOPT: An SQP algorithm for large-scale constrained optimization,” *SIAM Review*, vol. 47, pp. 99–131, 2005.
- [35] S. Boyd and L. Vandenberghe, *Convex Optimization*. Cambridge University Press, 2004.
- [36] S. Kim, K. Asadi, M. Littman, and G. Konidaris, “Deepmellow: Removing the need for a target network in deep Q-learning,” in *International Joint Conference on Artificial Intelligence*, 2019, pp. 2733–2739.
- [37] B. Gao and L. Pavel, “On the properties of the softmax function with application in game theory and reinforcement learning,” *arXiv:1704.00805*, 2017.

APPENDIX

A. Composition rule [35]

A composition of functions $f(g_1(\mathbf{z}), \dots, g_p(\mathbf{z}))$, where $f: \mathbb{R} \rightarrow \mathbb{R}$ is convex and $g_1, \dots, g_p: \mathbb{R}^q \rightarrow \mathbb{R}$, is convex when it satisfies the following composition rule. Let $\tilde{f}: \mathbb{R} \rightarrow \mathbb{R} \cup \{\infty\}$ be the extended-value extension of f . One of the following conditions must be met for each $i = 1, \dots, p$:

- i) g_i is convex and \tilde{f} is nondecreasing in argument i .
- ii) g_i is concave and \tilde{f} is nonincreasing in argument i .
- iii) g_i is affine.

The composition rule for concave functions is analogous.

B. Proof of Lemma 1

$$\text{mm}_k(\mathbf{a}) - \max(\mathbf{a}) = \frac{-\log(r) + \log(\sum_{i=1}^r e^{k(a_i - \max(\mathbf{a}))})}{k}. \quad (26)$$

Note that $1 \leq W \leq r$ where W is defined as $W := |\{a_i = \max(\mathbf{a}) : i \in \{1, \dots, r\}\}|$. We consider (26) for the case of the equality conditions of this inequality. When $W = r$, i.e., $a_1 = a_2 = \dots = a_r$, the left-hand side of equation (26) is equal to 0, which is the greatest value that the left-hand side can take because of the monotonicity of the log-sum-exp function as in Appendix F. Thus, we get $\text{mm}_k(\mathbf{a}) - \max(\mathbf{a}) \leq 0$. By taking a minus sign for the whole expression and a minus sign in front of each argument, we get $-\text{mm}_k(-\mathbf{a}) + \max(-\mathbf{a}) \geq 0$, that is, $\widetilde{\text{min}}_k(\mathbf{a}) - \min(\mathbf{a}) \geq 0$. Hence, the mellowmin function is an over-approximation of the true min.

On the other hand, when $W = 1$, the left-hand side of (26) is greater than $-\log(r)$, which is the bound we get, because of the monotonicity of the log-sum-exp. That is, $\text{mm}_k(\mathbf{a}) - \max(\mathbf{a}) \geq -\log(r)$. By taking a minus sign for the whole expression and a minus sign in front of each argument, we get inequality (19).

C. Proof of Theorem 4

From Lemma 1, for any STL formula φ in negation normal form (NNF),

- $\rho_{\text{rev}}^\pi((\mathbf{x}, t)) = \widetilde{\rho}_{\text{rev}}^\pi((\mathbf{x}, t))$
- $\widetilde{\rho}_{\text{rev}}^{\varphi_1 \wedge \varphi_2}((\mathbf{x}, t)) = \rho_{\text{rev}}^{\varphi_1 \wedge \varphi_2}((\mathbf{x}, t))$
- $\widetilde{\rho}_{\text{rev}}^{\varphi_1 \vee \varphi_2}((\mathbf{x}, t)) \geq \rho_{\text{rev}}^{\varphi_1 \vee \varphi_2}((\mathbf{x}, t))$
- $\widetilde{\rho}_{\text{rev}}^{\varphi_1 \square_{[t_1, t_2]} \varphi_2}((\mathbf{x}, t)) = \rho_{\text{rev}}^{\varphi_1 \square_{[t_1, t_2]} \varphi_2}((\mathbf{x}, t))$
- $\widetilde{\rho}_{\text{rev}}^{\varphi_1 \diamond_{[t_1, t_2]} \varphi_2}((\mathbf{x}, t)) \geq \rho_{\text{rev}}^{\varphi_1 \diamond_{[t_1, t_2]} \varphi_2}((\mathbf{x}, t))$
- $\widetilde{\rho}_{\text{rev}}^{\varphi_1 \mathbf{U}_{[t_1, t_2]} \varphi_2}((\mathbf{x}, t)) \geq \rho_{\text{rev}}^{\varphi_1 \mathbf{U}_{[t_1, t_2]} \varphi_2}((\mathbf{x}, t))$.

By induction, these inequalities follow that

$$\widetilde{\rho}_{\text{rev}}^{\varphi, k}(\mathbf{x}) \leq 0 \implies \rho_{\text{rev}}^\varphi(\mathbf{x}) \leq 0 \quad (27)$$

From this relation and (2), equation (20) follows.

D. Proof of Theorem 5

Recall from Lemma 1 that for $k \geq \frac{\log(r)}{\epsilon}$, we have

$$|\min(\mathbf{a}) - \widetilde{\min}(\mathbf{a})| \leq \epsilon. \quad (28)$$

By applying this inequality to the definition of $\widetilde{\rho}_{\text{rev}}^{\varphi, k}$ (7), we have

- $|\widetilde{\rho}_{\text{rev}}^\pi((\mathbf{x}, t)) - \rho_{\text{rev}}^\pi((\mathbf{x}, t))| = 0$
- $|\widetilde{\rho}_{\text{rev}}^{\varphi_1 \wedge \varphi_2}((\mathbf{x}, t)) - \rho_{\text{rev}}^{\varphi_1 \wedge \varphi_2}((\mathbf{x}, t))| \leq 0$
- $|\widetilde{\rho}_{\text{rev}}^{\varphi_1 \vee \varphi_2}((\mathbf{x}, t)) - \rho_{\text{rev}}^{\varphi_1 \vee \varphi_2}((\mathbf{x}, t))| \leq \epsilon$
- $|\widetilde{\rho}_{\text{rev}}^{\varphi_1 \square_{[t_1, t_2]} \varphi_2}((\mathbf{x}, t)) - \rho_{\text{rev}}^{\varphi_1 \square_{[t_1, t_2]} \varphi_2}((\mathbf{x}, t))| \leq 0$
- $|\widetilde{\rho}_{\text{rev}}^{\varphi_1 \diamond_{[t_1, t_2]} \varphi_2}((\mathbf{x}, t)) - \rho_{\text{rev}}^{\varphi_1 \diamond_{[t_1, t_2]} \varphi_2}((\mathbf{x}, t))| \leq \epsilon$
- $|\widetilde{\rho}_{\text{rev}}^{\varphi_1 \mathbf{U}_{[t_1, t_2]} \varphi_2}((\mathbf{x}, t)) - \rho_{\text{rev}}^{\varphi_1 \mathbf{U}_{[t_1, t_2]} \varphi_2}((\mathbf{x}, t))| \leq \epsilon$.

By induction, inequality (21) holds. A similar proof can be found in [5, 13].

E. Proof of Proposition 2

As [35, p. 88] and [36, Claim 1], the *mellowmax* function has the analytic form of Hessian:

$$\nabla^2 \widetilde{\max}_k(\mathbf{a}) = \frac{k}{(\mathbf{1}^\top \boldsymbol{\sigma})^2} ((\mathbf{1}^\top \boldsymbol{\sigma}) \text{diag}(\boldsymbol{\sigma}) - \boldsymbol{\sigma} \boldsymbol{\sigma}^\top) \geq 0 \quad (29)$$

where $\boldsymbol{\sigma} = [\sigma_1, \dots, \sigma_r]^\top$, $\sigma_i = e^{ka_i}$. Thus, this *mellowmax* function is convex when the parameter $k \geq 0$. By taking a minus sign for the whole expression and a minus sign in front of each argument, we get the Hessian of the *mellowmin*: $\nabla^2 \widetilde{\min}_k = -\frac{k}{(\mathbf{1}^\top (-\boldsymbol{\sigma}))^2} ((\mathbf{1}^\top (-\boldsymbol{\sigma})) \text{diag}(-\boldsymbol{\sigma}) - (-\boldsymbol{\sigma})(-\boldsymbol{\sigma})^\top) \leq 0$. Thus, the *mellowmin* function (18) is concave as long as $k \geq 0$.

F. Properties of max, min, and their smoothed functions

Convexity, monotonicity, and which approximation (over-approximation or under-approximation) of max, min, and their smoothed functions are summarized as follows.

- i) The max function is a nondecreasing convex function whereas its smooth approximations, i.e., the $\widetilde{\max}_k$ and function is a strictly increasing convex function.
- ii) The min operator is a nonincreasing convex function whereas its smooth approximations, i.e., $\widetilde{\min}_k$ function is a strictly decreasing concave function.

TABLE IV: Summary of each function's curvature and which approximation (over-approximation or under-approximation) is used when the parameter $0 < k < \infty$. Other smooth max functions are analogous.

function	curvature	approximation
max	convex	–
min	concave	–
$\widetilde{\min}_k$	concave	under-approx. of min
$\widetilde{\min}_k$	concave	over-approx. of min
$\widehat{\min}_k$	–	over-approx. of min

G. The simplification algorithm [8]

Algorithm 4 simplification(\mathcal{T}^φ)

Input: robustness tree $\mathcal{T}^\varphi = (\mathcal{O}, \mathcal{A}, \mathcal{S})$

Output: Simplified robustness tree

```

1: Flag = True
2: while Flag do
3:   Flag = SIMPLIFYONCE( $\varphi$ )
4: function SIMPLIFYONCE( $\Phi$ )
5:   Flag=false
6:   for each  $i$  in  $\{1, \dots, n\}$  do
7:     if subtree  $\mathcal{T}^{\Phi_i}$  is not a predicate then
8:       if  $\mathcal{O}^\Phi = \mathcal{O}^{\Phi_i}$  then
9:          $\mathcal{A}^\Phi$ .pop( $i$ ) (removes  $i$ -th tree  $\mathcal{T}^{\Phi_i}$ )
10:         $\mathcal{S}^\Phi$ .pop( $i$ ) (removes  $i$ -th timestep  $t^{\Phi_i}$ )
11:         $\mathcal{A}^\Phi \leftarrow \mathcal{A}^\Phi \parallel \mathcal{A}^{\Phi_i}$ 
12:         $\mathcal{S}^\Phi \leftarrow \mathcal{S}^{\Phi_i} + t^{\Phi_i}$  (elementwise plus  $t^{\Phi_i}$ )
13:         $\mathcal{S}^\Phi \leftarrow \mathcal{S}^\Phi \parallel \mathcal{S}^{\Phi_i}$ 
14:       Flag=True
15:       Flag = Flag  $\vee$  SIMPLIFYONCE( $\mathcal{T}^{\Phi_i}$ )
16: Return Flag

```
